Annu. Rev. Astron. Astrophys. 1998. 36:539–98

MODELING EXTRAGALACTIC JETS

Attilio Ferrari
Dipartimento Fisica Generale, Università di Torino, Via Giuria 1, I-10125 Torino, and Osservatorio Astronomico di Torino, I-10025 Pino Torinese, Italy;
e-mail: ferrari@to.astro.it

KEY WORDS: galactic nuclei, radio astronomy, astrophysical fluid dynamics

ABSTRACT

Extragalactic jets were discovered and initially studied by radio astronomers in connection with extended radio sources. At present, the combination of jets and disks is considered the crucial element in unification models for all active galactic nuclei (AGNs). The acceleration and propagation conditions of jets, together with the aspect ratio of the disk/jet geometry with respect to the observer, shape the morphologies of AGNs. However, these phenomenological models are very complex from the physical and mathematical point of view, as they involve different elements of the theories of gravitation, fluid dynamics, and electrodynamics in a highly nonlinear combination and in conditions not easily reproducible in laboratory plasma or fluid experiments. In the last ten years, theorists have attacked the subject with advanced analytical and numerical methods, and some important results have already been established that confirm the global scenario, although we are still far from a complete physical interpretation. This review summarizes the main results on the art of jet modeling, emphasizing the limitations of the available models and the possibility of new developments.

1. HISTORICAL INTRODUCTION

The evidence for highly collimated jets in astrophysics goes back to the early radio observations of twin lobes in extended radio galaxies, of which the prototype is Cygnus A (Jennison & Das Gupta 1953). After associating them with optical galaxies at cosmological distances, it was clear that they had gigantic dimensions (up to megaparsec scales) and astonishing powers (up to 10^{47} erg s^{-1}) emitted as nonthermal radio continua of synchrotron type. These facts made a single ejection event from the nucleus of the parent galaxy

0066-4146/98/0915-0539$08.00

unlikely and, in general, posed a serious energetic problem (Burbidge 1958). In fact, the stopping distance of a plasmon moving in a constant density environment is $D \sim s/\nu$, where s is the plasmon scale and ν the density ratio environment/plasmon. Unless dense plasmons are considered, which would then require high kinetic energy for their ejection (up to $\geq 10^{61}$ erg), the typical geometry should display $D \leq s$, in contrast with observations. The same amount of energy delivered continuously on times $\geq 10^7$ years by supersonic outflows (with $v_s \ll v_j$ so that $s \ll D$) is a less severe problem (Rees 1971, Scheuer 1974).

In addition, the short synchrotron lifetimes of relativistic electrons do not allow radio emission for more than $\sim 10^6$ years unless reacceleration is introduced to the picture, and the situation is obviously much worse for higher frequencies. Again, this phenomenology could be explained more economically in terms of fluid jets continuously transferring energy and momentum from the galactic nuclei into the lobes and maintaining "in situ" particle reacceleration (Blandford & Rees 1974).

Finally, with the increase in sensitivity and angular resolution of radio telescopes, bridges of nonthermal emission were detected connecting galactic nuclei and radio lobes (see e.g. Miley et al 1975, Turland 1975, Bridle & Fomalont 1976, van Breugel & Miley 1977); a complete summary is given by Miley (1980). Although nonthermal continua did not allow Doppler measurements of velocities in these bridges, it was clear that a permanent physical link existed between nuclei and lobes characterized by a surprising collimation.

Very long baseline interferometry (VLBI) observations traced the outflow collimation down to subparsec scales and allowed measurements in several cases of superluminal proper motions (Cohen et al 1971, Moffet et al 1971, Whitney et al 1971). This fact, together with a statistically significant presence of one-sided jets in strong sources, was considered evidence that jets may, at least in some cases, be relativistic.

Eventually jets were discovered to emit also in the optical, X-, and γ-ray bands, and their relationship with very high-energy phenomena originating in the deep cores of active galactic nuclei (AGNs) was definitively established. In this respect, three recent observational developments must be mentioned:

1. The Hubble Space Telescope (HST) has gathered clear evidence of a close-spatial connection between thermal and nonthermal radiation emissions in the central regions of some AGNs; in particular, the nonthermal emission corresponds to the initial part of the jet that appears to compress the external interstellar plasma while ploughing its way out (Capetti et al 1996).

2. The Compton Gamma-Ray Observatory (CGRO) has detected strong and highly variable γ-ray emission from blazars, suggesting that these objects

Table 1 Estimated physical parameters

Active galactic nuclei (AGN) powers	10^{39}–10^{49} erg s^{-1}
Variability time scales	Hours to years
Jet lengths	<1 pc to few megaparsecs
Relativistic jet Lorentz factors	10–10^3

owe their enormous brightness to relativistically Doppler-boosted radiation from jets pointing toward the Earth (Hartman et al 1992).

3. Monitoring of intraday/intranight variability of blazars supports the idea that beaming of jets with Lorentz factors as high as 10^3 can explain their huge energetics and rapid time scales of variability (Witzel 1992); however, coherent radiation mechanisms could partly reduce this request.

Table 1 summarizes the characteristic physical parameters of AGNs and their jets. Figure 1 is a representative collection of sample morphologies.

In this framework, modeling of supersonic, relativistic, collimated outflows from AGNs has been one of the most challenging problems in astrophysics in recent years. The early development of the numerical study of supersonic hydrodynamic and magnetohydrodynamic flows has been connected with the observations of the solar and stellar winds and plasma motions in solar magnetic loops. Although the global and specific energetics of stellar and galactic phenomena differ by orders of magnitude, most of the dynamical events and the underlying physical processes may not be conceptually far apart. In this review, we discuss the present state of the theoretical modeling of jets while highlighting the results commonly accepted as definitive and the problems that are still open.

For detailed analyses of existing data on jets, from radio to high frequencies, we refer to the many published reviews, first of all those that appeared in this series by De Young (1976), Miley (1980), Kellermann & Pauliny-Toth (1981), and Bridle & Perley (1984). Recent HST optical data are presented by Macchetto (1996) and high-frequency data by Hartman et al (1992). The physical parameters of jets are commonly derived under the assumption they are "optically thin incoherent synchrotron sources." In particular, with an eye to the energy budget, estimates are made in the assumption of minimum energy requirement corresponding to equipartition between relativistic electrons (and protons or positrons) and magnetic fields (Burbidge 1958). For the cores, the optically thin approximation breaks down and other models are used. Further estimates can be done using polarization, depolarization, and Faraday rotation measures. Using these diagnostics, typical average physical parameters of extended radio galaxies can be obtained (Table 2).

2. THE PHENOMENOLOGICAL MODEL

Because VLBI measurements of proper motions in the compact regions of jet formation favor flow velocities that are very close to the speed of light, it appears that jet acceleration is a highly relativistic process that takes place in the vicinity of a gravitational horizon. In addition, since a high degree of collimation is observed in jets, confinement is required. The most obvious agent is pressure

(*a*)

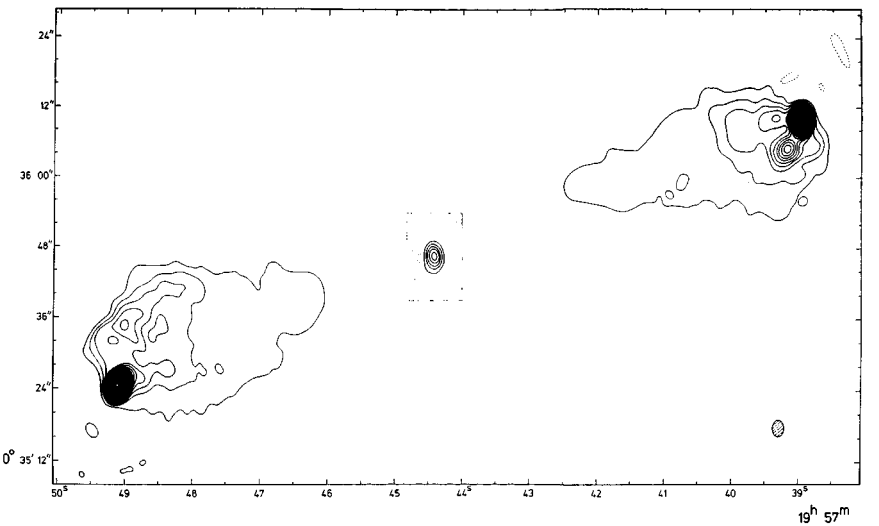

(*b*)

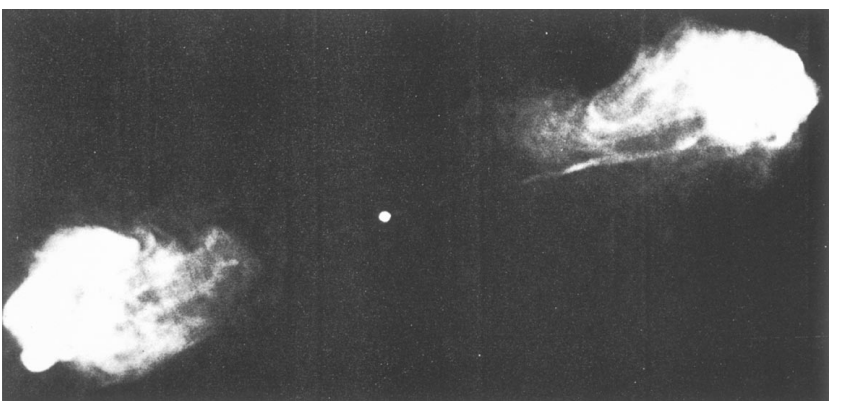

Figure 1 Collimated jets from active galactic nuclei (AGNs): (*a*) Cygnus A in early observations; (*b*) VLA radio map of Cygnus A.

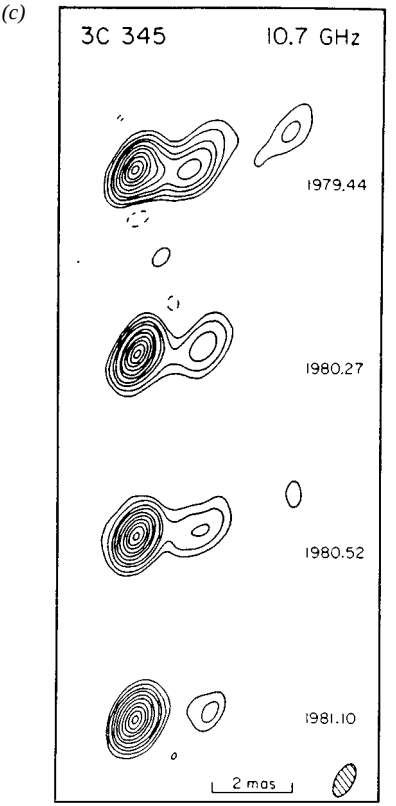

Figure 1 (*Continued*) (*c*) Superluminal motions in 3C 345.

by an external medium and/or magnetic field. Typical plasma parameters of the ambient surrounding radio galaxies are listed in Table 3.

The measurements of the ambient pressures come from the low angular resolution X-ray surveys of the regions around radio jets, but they are still relatively scarce. Structures in strong jets appear to be often overpressured (Bicknell & Begelman 1996), while weak jets are always underpressured or in pressure equilibrium (Feretti et al 1995). Obviously, observed features may in fact be transients.

The standard synchrotron plasma model requires that radio-emitting regions contain a suprathermal electron gas that coexists with a cold component (protons and nuclei) that dominates the mass content. Some authors have suggested that outflows are made of electron-positron pairs (with and without a proton-electron

(d)

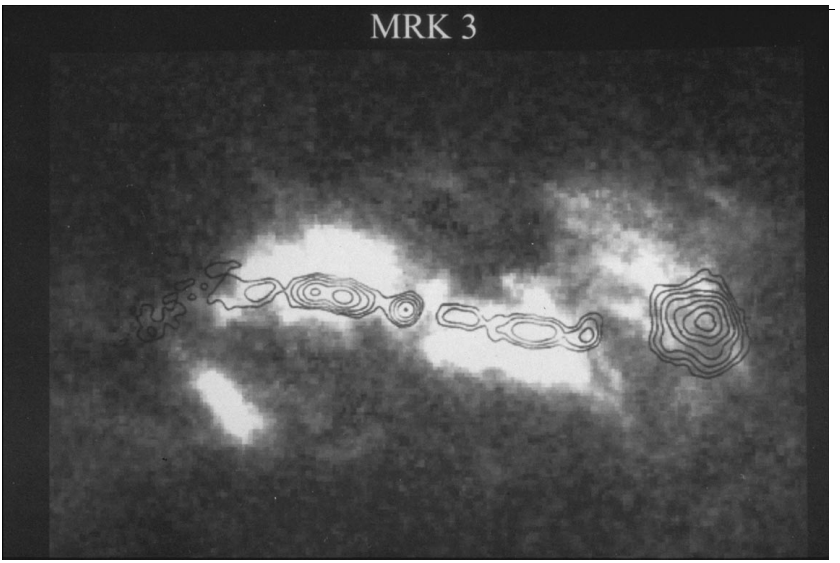

(e)

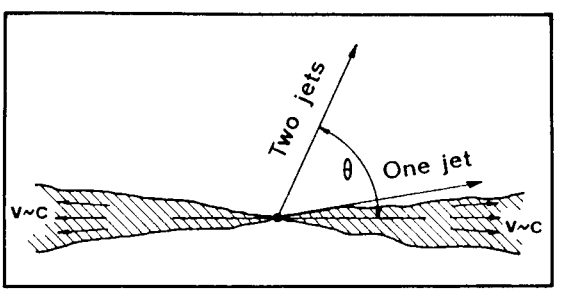

Figure 1 (*Continued*) (*d*) Hubble Space Telescope (HST) map of Markarian 3 (Capetti et al 1996); and (*e*) geometry of Doppler beaming in one-sided jets and blazars.

component) in order to explain the fact that energy is not deposited along jets and to reduce the kinetic energy content in radio lobes (Bicknell & Begelman 1996, Kundt 1996).

A few considerations are worth mentioning in connection with this picture. The first is about the observed morphologies of magnetic fields, as derived from polarized emissivity measurements. Continuous emission comes from discrete structures as knots and filaments that may not be in steady pressure equilibrium, and they may not even be in equipartition conditions but transient. In addition, they lower the emission filling factor and reduce the energy budget.

Table 2 Radio galaxies

	Core	Jet	Hot spot	Lobe
D (size) (kiloparsecs)	$\leq 10^{-3}$	2–10^3	5	50–10^3
B_{eq} (Gauss)		$\leq 10^{-3}$	10^{-3}	10^{-5}
$n_{e,rel}$ (cm^{-3})		10^{-2}–10^{-5}	$\leq 10^{-2}$	$\leq 10^{-4}$
Polarization (%)	≤ 2	0–60	15	0–60
Spectral index (α)	0.0	0.6	0.6	0.9
v_{flow}/c	$\rightarrow 1$	10^{-1}	10^{-3}	10^{-3}

Second, the early proposal of an adiabatic expansion of emitting structures (blobs) along the jet that would make emissivity critically dependent on the source projected cross section [$\propto r^{-(5+4\alpha)}$, α spectral index] is not verified by observations (Scheuer 1974). Thence either turbulent amplification of magnetic fields occurs everywhere, or transient formations dominate the dynamics.

2.1 *Phenomenology of an Extended Radio Source*

The original phenomenological model was proposed by Rees (1971) and Scheuer (1974). A pictorial scheme is illustrated in Figure 2. Twin opposite jets are produced and collimated in the innermost cores of AGNs (sizes $\leq 10^{-3}$ pc) by some powerful engine that most likely derives its energy from accretion onto a gravitational well and thrusts continuously supersonic and/or super-Alfvènic magnetized plasma along the angular momentum axis. The twin jets plough their way through the ambient intergalactic gas, transferring energy and momentum far away from the parent core. Jets are structurally affected by the interaction with the external medium originating shocks, filaments, and wiggles. Local electron acceleration to relativistic energies supports synchrotron emission. The "head" where the jet pushes against the external medium is a turbulent working surface producing a bow shock and a cocoon around the entire source.

The physical modeling of this scenario is difficult because of the high nonlinearities involved, including electrodynamic and general relativistic effects. Various building blocks of the overall model have been attacked. In particular, the following sections of this review address the main physical questions related with jets: (*a*) origin, acceleration, and collimation, (*b*) propagation and confinement, (*c*) termination, and (*d*) radiation.

Table 3 The ambient medium of radio galaxies

n_{th} (cm^{-3})	10^{-4}–10^{-3}
T (K)	2–3×10^7
B (Gauss)	$<10^{-6}$–10^{-5}

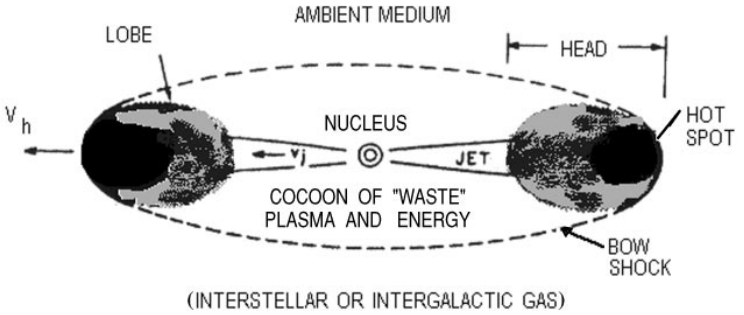

Figure 2 Schematic diagram of a strong radio source.

When describing the structure and dynamics of outflows, a fluid approximation is used, assuming that magnetic fields provide a collective behavior even though the particle collisional mean-free-path λ_{coll} is very large ($\lambda_{gyr} \ll D \ll \lambda_{coll}$, where λ_{gyr} is the gyration radius and D the region size). It is not clear what the field-filling factor is in the various regions and how important the turbulent versus the ordered magnetic component is. However, they are both essential for radiation and dynamics: In particular, fluid models must use magnetohydrodynamics.

2.2 *Jets and Unified Models for Active Galactic Nuclei*

Jets appear to be characteristic ingredients of all AGNs. Phenomenological scenarios in which Seyfert galaxies, radio galaxies, quasars, and blazars are interpreted as different manifestations of the same type of central power engine, with different powers and geometries, have become very popular. Some useful general references are the reviews by Blandford et al (1990), Antonucci (1993), and Falcke (1996).

The key elements in these unification models are an unresolved accretion disk on scales $\ll$1 pc and the twin opposite jets that are accelerated perpendicular to its plane: The jet /disk orientation with respect to the observer defines the visibility of the spectral components. In particular, jets are fully visible when they are perpendicular to the observer's line of sight, which is the case of extended radio galaxies and radio-loud quasars. Instead, jets are not clearly distinguishable when they are seen face-on, but correspondingly, their emission is relativistically Doppler boosted in frequency and luminosity, which is the case of blazars and compact radio galaxies. Weak AGNs would produce small jets, and the above classes would become Seyfert 2 (large angles to the line of sight), Seyfert 1 (smaller angles), and BL Lacs (face-on).

On scales on the order of parsecs, the accretion flow takes the form of a thick molecular torus that, depending on the orientation to the line of sight,

can substantially obscure the inner engine. For lines of sight close to the torus equatorial plane, the central engine becomes completely invisible: The only visible components of AGNs are then the radio jets.

Along this scheme, and starting from the original classification of extended radio galaxies in strong jets ($P_{178\mathrm{MHz}} > 5 \times 10^{25}$ W Hz^{-1}) and weak jets ($P_{178\mathrm{MHz}} < 5 \times 10^{25}$ W Hz^{-1}) by Fanaroff & Riley (1974), two basic unification sequences have been proposed originally for radio-loud objects: (*a*) the sequence of radio galaxies with strong jets (FR II objects) → quasars → blazars, in which obscuration of the central engine decreases and beaming increases; and (*b*) the sequence of radio galaxies with weak jets (FR I objects) → BL Lacs, in which again obscuration of the central engine decreases and beaming increases. Similarly, radio-quiet objects were unified in a third sequence of Seyfert 2 → Seyfert 1 → radio-quiet BL Lacs.

However, the original classification in two categories of radio-loud and radio-quiet AGNs is now overruled by more sensitive observations that indicate how a radio component is present in all cases, although with different powers. The more appropriate classes of radio-loud and radio-weak AGNs should now be used (Antonucci 1993). Therefore, Falcke & Biermann (1995) and Falcke et al (1995) have analyzed the influence of the power of the central engine on morphologies in order to unify the above sequences. They found, in fact, a significant correlation between the ultraviolet-bump luminosity, taken as a measure of the disk (engine) luminosity, and the radio luminosity of the three sequences of AGNs. The radio-loud objects in fact do constitute a sequence going from FR I to FR II, quasars and blazars for increasing disk power, whereas radio-weak objects follow the same pattern at lower radio luminosity.

In particular, increasing the disk power produces stronger radio jets. Their emission is related mainly to internal relativistic electron acceleration. However, an important component in the initial propogation comes from the interaction of the collimated flows with the walls of the large-scale torus, leading to enhanced particle acceleration. The stronger the jet-torus interaction, the more prominent the jets. If the opening angle of the torus is assumed to be power dependent so that less powerful jets have narrower opening angles and suffer weaker jet-torus interaction, then this would explain the observational results that jets are systematically more prominent with decreasing radio power.

Finally, the difference between the radio-loud and radio-weak objects would be related to the fact that the first ones are produced by ellipticals and the latter by spirals. In this last case, the jets always would be weaker for the same central engine power and would suffer strong interaction with the external torus.

Given the simplicity of these arguments, Falcke et al (1995) suggested that observations support the idea that all AGNs have the same type of central engine, with their different morphologies produced by obscuration, beaming,

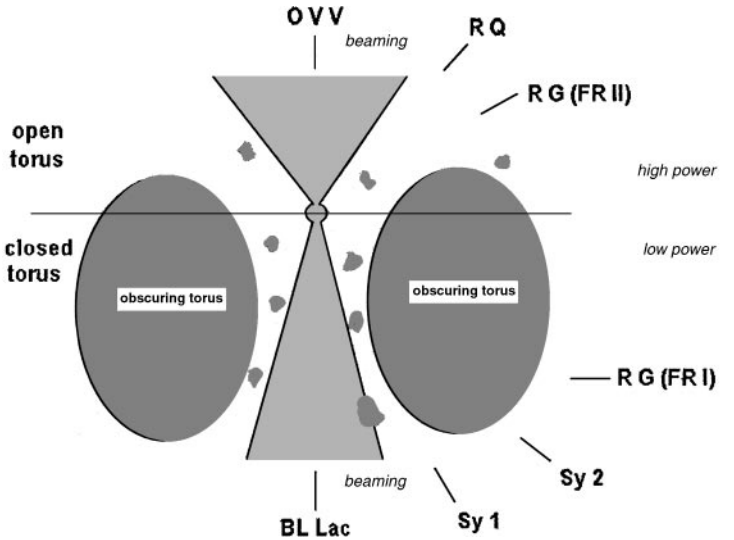

Figure 3 A unified model of AGNs. The *upper part* of the drawing corresponds to high-power sources with the jet emerging from an open torus, the *lower part* to low-power sources with the jet emerging from a closed torus. Different morphologies are produced by the orientation of the observer with respect to the jet/obscuring torus. OVV, optically violent variables; RQ, radio-loud quasars; RG, radio galaxies; Sy, Seyfert galaxies.

and power. Incidentally, they also proved that the same correlation holds for stellar mass black holes with superluminal jets (Mirabel & Rodriguez 1994). A sketch of this classification is given in Figure 3.

3. ORIGIN OF JETS: THE BLACK HOLE CONNECTION

The phenomenology of AGNs, namely their exceedingly large powers (up to 10^{47} erg s^{-1}) and concentration in small volumes ($\leq 10^{-3}$ pc), leads to consideration of models for jet formation based on processes around supermassive black holes ($M \geq 10^7\ M_\odot$) (Rees 1984). Other suggested origins, namely star clusters, pulsar clusters, and spinars, appear to be inadequate to explain the total power, the long-term stability of quasars and radio galaxies, and short-term variability. The launch and collimation of supersonic (eventually relativistic) outflows from supermassive black holes can originate from two distinct mechanisms: (*a*) accretion of matter onto the black hole, liberating gravitational binding energy that is transferred to matter flung along the rotational axis; (*b*) electrodynamic processes, tapping black hole rotational energy and feeding

it into large-scale magnetic fields. In both cases, the global picture leads to the formation of twin opposite jets as in the early proposal by Blandford & Rees (1974).

3.1 *Collimated Outflows from Accretion Disks*

The structure of gaseous, magnetized or unmagnetized disks is reviewed by Papaloizou & Lin (1995). Two characteristic configurations can be obtained analytically by solving the structure equations: (*a*) thin disks and (*b*) thick disks or tori, depending on whether the energy dissipated into the plasma by stresses can be rapidly radiated away or if the local pressure is competitive with gravity instead (Begelman et al 1984). In both cases, the activity at the disk surface creates a hot corona that drives winds along the rotation axis.

HYDRODYNAMIC WINDS Hot matter at the surface of a disk can be accelerated outwards against the gravitational pull of a compact core of mass M_h by hydrodynamic pressure forces. This idea was first applied to jet acceleration by Blandford & Rees (1974) in the twin-exhaust model whose physics is derived from the stellar wind theory. Among the many subsequent papers, we refer to Fukue & Okada (1990), who presented a complete axisymmetric solution of the balance equations along and perpendicular to streamlines (Bernoulli and Grad-Shafranov equations, respectively), also including the effect of centrifugal forces generated by the disk rotation. In cylindrical geometry (r, ϕ, z) with ds as a line element along a streamline and dn perpendicular to it, these equations are

$$\frac{1}{\rho}\frac{dp}{dn} = -\frac{GM_h}{(r^2+z^2)^{3/2}}\frac{rdz - zdr}{ds} + \frac{L^2}{r^3}\frac{dr}{ds}; \tag{1}$$

$$v\frac{dv}{ds} + \frac{1}{\rho}\frac{dp}{ds} = -\frac{GM_h}{(r^2+z^2)^{3/2}}\frac{rdr + zdz}{ds} + \frac{L^2}{r^3}\frac{dr}{ds}, \tag{2}$$

where L is the specific angular momentum. Energy is injected into each streamline at the base on the disk, and a flow pattern is set up that crosses transonic surfaces to produce a supersonic wind. If the temperature distribution on the disk is flatter than $1/r_e$ (r_e is the equatorial distance), the gas ejected into streamlines close to the axis is gravitationally confined and forms a corona, while the gas on external streamlines can form a wind. The opposite is true for a temperature distribution steeper than $1/r_e$. These two patterns correspond to hollow jets and well-collimated jets, respectively. The flow goes through multiple critical points, passing from subsonic to supersonic and vice versa several times with formation of shocks. The novelty of these solutions with respect to the original twin-jet model is the possibility of studying the wind solution stability and especially of bringing the first critical point very close

to the core and immediately making the jet supersonic, as is observed. The link between jets and disks in the hydrodynamic models is only through the injection of energy at the base of streamlines. There is no direct back-reaction from the jets to the disk.

MAGNETOHYDRODYNAMIC WINDS Magnetohydrodynamic (MHD) winds are an important source of advection losses from disks; they occur in the presence of an initial poloidal magnetic field anchored in the accreting material that is wound up by rotation of the disk and generates a collimating toroidal field. Thus accretion disks can naturally drive winds by centrifugal or magnetocentrifugal mechanisms (Mestel 1961, Weber & Davis 1967, Sakurai 1985). The set of MHD nonlinear partial differential equations is

$$\nabla \cdot \mathbf{B} = \nabla \cdot (\rho \mathbf{v}) = \nabla \times (\mathbf{v} \times \mathbf{B}) = 0; \tag{3}$$

$$\rho(\mathbf{v} \cdot \nabla)\mathbf{v} - (\mathbf{B} \cdot \nabla)\frac{\mathbf{B}}{4\pi} = -\nabla\left(P + \frac{B^2}{8\pi}\right) - \rho\nabla\Phi; \tag{4}$$

$$\rho\mathbf{v} \cdot \left(\nabla\mu - \frac{1}{\rho}\nabla P\right) = \rho\sigma, \tag{5}$$

where μ is the specific enthalpy and σ the specific heating/cooling rate. Steady-state solutions for the full two-dimensional (2-D) problem of jet acceleration from accretion disks exist for the axisymmetric case only. In this case, the set of MHD equations can be reduced to two coupled equations, the Bernoulli and Grad-Shafranov (or transfield) equations, which fully describe the wind dynamics along and across streamlines, respectively. However, these equations are formidably difficult, and some simplifying assumptions must be adopted. The main problem encountered is the presence of several critical points where equations become singular. Physically acceptable solutions must go through these points smoothly. In one-dimensional geometries, they correspond to the flow reaching the characteristic propagation speeds in the fluid (Alfvènic, slow, and fast magnetosonic); in 2-D geometries, this is no longer true for the bulk velocity but applies to specific velocity components (Tsinganos et al 1996).

Self-similar solutions: the Blandford & Payne model The seminal paper in the context of magnetized disks and jets is by Blandford & Payne (1982), who found self-similar steady-state solutions of the ideal MHD equations of a cold, axially symmetric magnetospheric flow from a Keplerian disk. They assumed that the disk is threaded by open poloidal magnetic field lines corotating with the disk at the Keplerian velocity; in cylindrical coordinates (r, ϕ, z),

$$\mathbf{B} = (\mathbf{B}_r, \mathbf{B}_\phi, \mathbf{B}_z), \quad \mathbf{B}_p \equiv (\mathbf{B}_r, \mathbf{B}_z) = \frac{1}{r}\left(-\frac{\partial\psi}{\partial z}, \frac{\partial\psi}{\partial r}\right), \tag{6}$$

where ψ is the flux function. Total magnetic field lines are wrapped around ψ = constant magnetic surfaces. Matter is centrifugally driven outwards in the corona and is frozen along field lines $\mathbf{v} = k\,(\psi)\,\mathbf{B}_p/4\pi\rho + r\omega(\psi)\hat{\phi}$, where k is a structure constant and ω the angular velocity; k and ω are related as $(\mathbf{B}\cdot\nabla)k = (\mathbf{B}\cdot\nabla)\omega$. The second term implies that a toroidal field is generated:

$$\mathbf{B} = \mathbf{B}_p + B_\phi\hat{\phi}, \tag{7}$$

which becomes dominant at large radii close to the rotation axis and consequently collimates the flow into a jet. The self-similar solutions are obtained with scaling in terms of the radial distance from the center:

$$\mathbf{r} = [r_0\xi(\chi), \phi, r_0\chi], \quad \mathbf{v} = [\xi'(\chi), g(\chi),\ f(\chi)]\left(\frac{GM}{r_0}\right)^{1/2}. \tag{8}$$

For a fixed colatitude $\theta = \mathrm{z}/r$ (i.e. same χ), all physical quantities scale with the spherical radius, and the MHD equations reduce to a second-order differential equation in χ for the Alfvènic Mach number v/v_A, $v_A = (B^2/4\pi\rho)^{1/2}$, and a first-order equation for the field/streamline geometry. Both equations have singular points and are studied with the above-mentioned technique of wind solutions. Physical solutions must cross singular points with regularity; the study of the topology of these critical points is rather involved and defines the characteristics of solutions. In fact, the Blandford & Payne solutions are not imposed to cross the fast magnetosonic point, and this causes a collapse of the solutions on the symmetry axis at large distances (eventually at infinity).

Blandford & Payne found two classes of collimated wind solutions depending on the final flow velocity: (*a*) fast magnetosonic winds with paraboloidal asymptotic streamlines and (*b*) trans–fast-magnetosonic winds that focus onto the rotation axis. In the first class about one third of the energy is carried as bulk kinetic energy and two thirds as Poynting flux; the second class is instead dominated by the kinetic flux and in this sense is very interesting, although it has the drawback of an excess of pinching force corresponding to a divergence in the electric current on the axis. Far from the axis, the flow continues its free expansion and is instrumental in extracting angular momentum from the system by magnetic torque. Even a small mass loss can carry a large specific angular momentum given the large lever arm of the field acting on the matter.

Other radial self-similar solutions have been studied by Contopoulos & Lovelace (1994), Pelletier & Pudritz (1992), and Rosso & Pelletier (1994). In particular Contopoulos & Lovelace derived a relation between the shape of streamlines and the poloidal current consistent with the magnetic structure. Also, the Blandford & Payne model has been extended to the special relativistic case by Li et al (1992), which shows that a kinetic energy flux comparable to the Poynting flux can be obtained. Contopoulos has proposed a steady solution for

jets without imposing an original poloidal field (Contopoulos 1995). A toroidal component originally present in the disk is increased by differential rotation. The strong pressure gradient between the disk (large B_ϕ) and the corona above it ($B_\phi \simeq 0$) ejects plasma perpendicular to the disk. For this to happen, the vertical velocity at the surface of the disks must be comparable to the Keplerian velocity $v_{z0} \sim v_{\phi 0}$. The ejected plasma convects azimuthal magnetic field and is self-collimated.

A different type of scaling has been proposed by Tsinganos, Trussoni, and Sauty (Sauty & Tsinganos 1994, Trussoni et al 1996, Tsinganos et al 1996), in which latitudinal self-similarity is used with all physical quantities expressed in separable form. In particular, the magnetic potential is written as

$$\psi(r,\theta) \propto f(r)g(\theta), \quad \text{with} \quad g(\theta) = \sin^2\theta, \tag{9}$$

and the Bernoulli and Grad-Shafranov equations for $f(r)$ are obtained. This scaling permits a better representation of the regions around the rotation axis of the system that are singular in the Blandford & Payne solution. Solutions correspond to super-Alfvènic winds, and one class provides self-confined outflows: After an initial quasi radial expansion, poloidal streamlines undergo some oscillations and then settle into a cylindrical pattern. Also note that these solutions do not require the use of a polytropic equation of state; in fact, they correspond to a given profile of the streamlines in θ, which fixes the profile of the propagation channel. The heating/cooling conditions to maintain the outflow (i.e. the local equation of state) can be derived a posteriori from the solutions, in order to determine whether they are physically reproducible.

Another class of MHD winds is based on simplifying the Grad-Shafranov equation, with the consequence, however, that solutions are valid only in restricted regions. For instance, close to the equatorial plane, the flow can be modeled in thin cylindrical shells by averaging physical quantities in the direction perpendicular to the axis (Lovelace et al 1991).

Persistence of the bead-on-wire configuration The connection between disks and jets is through the transfer of angular momentum. This allows the stability of disks and is the driving element for the spontaneous initiation of outflows. However, the field structure must be maintained in conditions to have flux lines inclined at 60° or less to the disk plane. Advection of field lines by supersonic mass flow tends to increase the inclination angle; resistive or ambipolar diffusion has been proposed to balance this effect, but in fact the angle is likely to move very close to 90° (Königl 1989, 1994). Consequently other ways must be found to launch and maintain a wind.

Ferreira & Pelletier (1993a,b, 1995) have shown that, taking into account viscous and magnetic turbulent effects in the disk plasma, the disk magnetic

pressure develops a vertical component that pushes matter to the surface, leading to a continuous transition from the resistive plasma disk to the ideal MHD jet.

Shu et al (1994) have proposed that MHD winds exist only along field lines originating from the inner edge of the disk, where the central object field lines penetrate into the disk and almost corotate with it: The corotation radius is $R_{cor} = (GM/\Omega_{star}^2)^{1/3}$. The disk is actually truncated inside this radius, as matter diffuses across the magnetic field (by microscopic mechanisms of ambipolar diffusion and ohmic dissipation), bends its lines inward, and accretes onto the central object. Also outside R_{cor}, matter diffuses onto field lines but bows them outward, transferring angular momentum to the disk, which can then reach super-Keplerian velocities and reaches an ideal configuration to start a funnel flow. This mechanism is referred to as magnetocentrifugal acceleration. For large accretion rates, the corotation radius moves close to the central object, which is forced to rotate at breakup conditions.

Recently, Contopoulos (1996) initiated the study of general solutions for axisymmetric flows without imposing $E_\phi = 0$, i.e. the poloidal velocity parallel to the poloidal magnetic field. This condition allows the magnetic field to be advected by the accretion flow and accumulated onto the axis of symmetry.

Relativistic flows Camenzind (1986) has pointed out that, when dealing with fast rotators and a strong gravitational field, use of the full machinery of the general relativistic MHD theory is unavoidable. Relativistic winds have the same critical points as the nonrelativistic ones: slow magnetosonic, Alfvènic, and fast magnetosonic points. A wind equation can be obtained along the flux tube. Camenzind showed that up to ∼80% of the initial Poynting flux at the base of the flux tube is converted into kinetic energy beyond the light cylinder and the wind velocity reaches Lorentz factors up to $\gamma_{bulk} \sim 8$. A current I is carried by the wind and is essentially determined by the total angular momentum lost through the outflow.

Radiation pressure acceleration Radiation-supported thick accretion disks have been studied for a way to stabilize them against the Papaloizou & Pringle instability (Frank 1979, Meier 1979). In addition, deep funnels, replenished by ultraviolet photons from the walls with a net outward momentum component, produce bulk acceleration of a wind by radiation pressure. Ferrari et al (1985) discussed the quasi–2-D hydrodynamic problem of relativistic equilibrium flows for given profiles of the propagation channels. Solutions exhibit many critical points. In particular, the sudden expansion at the exit of the funnel brings the first critical point close to the nucleus. The jet thrust is not constant but decreases in the subsonic regime and increases in the supersonic regime. In fact, the surface of the jet is not parallel to the flow, and this corresponds to an external pressure force acting consistently on the field. Where the channel

narrows (widens), the flow slows down (accelerates). Nobili (1998) consistently solved the radiation transport equation in the funnel, extending the results to the optically thick case. In all models related to acceleration by radiation pressure, the critically limiting factor is Compton drag by the same radiation. Particles moving at large velocities along the funnel overtake the photons emitted by the walls and have strong Compton losses. In fact, the asymptotic flow velocity cannot exceed a Lorentz factor $\gamma_{bulk} \leq 2$. A solution to this problem has been proposed by Ghisellini et al (1990), who considered the possibility that clouds of electrons in the flow can synchrotron self-absorb the radiation from the disk or funnel. In this case, absorption is selective so that red-shifted photons fall below an absorption cutoff and therefore cannot brake the flow. Lorentz factors up to $\gamma_{bulk} \sim 10$ are attained.

3.2 *Electromagnetic Winds from Black Hole/Disk Magnetospheres*

Blandford (1976) and Lovelace (1976) were first to discuss the generation of electromagnetic winds from force-free magnetospheres above thin accretion disks. They found that the rotation of the disk causes the magnetic lines to sweep the ambient plasma, which consequently feels a strong induced poloidal electric field. Correspondingly, as the magnetic field that is predominantly toroidal at large distances has a poloidal component, momentum and energy are carried away by an electromagnetic Poynting flux. The poloidal component of this flux lies on paraboloidal surfaces, and consequently, energy is focused on the rotation axis and carried away along it as an electromagnetic wind. In addition, a closed electric circuit is set up with a radial current flowing outward in the disk plane and an axial current flowing in along the rotation axis. This axial current can be initiated by a flow of relativistic electrons. At large distances, an ambient plasma can absorb the Poynting flux and give rise to particle jets. The ultimate energy source is rotation.

An important class of electromagnetic models considers Kerr black holes immersed in a large-scale magnetic field maintained by external sources (e.g. by currents in an accretion disk), whose flux is assumed to thread in part the event horizon. The basic picture is that matter inflowing onto the hole with large angular momentum carries a component B_z of a magnetic field parallel to the rotation axis. The configuration becomes analogous to the unipolar inductor proposed by Goldreich & Julian (1969) for pulsars and supports ejection of Poynting flux and relativistic plasma along open field lines (Phinney 1982).

Blandford & Znajek (1977), Macdonald & Thorne (1982), and Phinney (1982) examined a model of rotational energy extraction from Kerr black holes looking for a direct link with the properties of black holes. A way to extract this energy is to assume that magnetic flux lines threading the event horizon

originate from an electric potential difference between the poles and equator of the hole that causes a current to flow. For a 10^8 $M_\odot$ hole and a 10^4 G magnetic field, this potential difference can be as large as 10^{20} V. So large potentials do allow the production of electron-positron pairs by vacuum breakdown and maintain currents $\sim 10^{18}$ Amp from the horizon to infinity. A steady-state solution has been derived by Phinney (1982) in which two winds emanate from a source region inside the magnetosphere: a wind of charges falling into the hole and another moving outward. This last can be seen as a relativistic MHD wind where energy is mostly transported by Poynting flux. The main difference between this model and those of Blandford and Lovelace is that a black hole is a very good conductor with an electric resistance of $\sim$100 ohm. The magnetic coupling between the hole and the magnetosphere extracts work from the hole that is equal to the back-reaction from the magnetosphere to the hole plus the ohmic dissipation in the external load (magnetosphere and disks). The model is still controversial. Punsly & Coroniti (1990) have pointed out that the ingoing wind must flow faster than any MHD wave signal, and therefore the event horizon is fundamentally without a causal contact with the source region and the outgoing wind itself. Blandford (1989) has proposed that the causal connection can be established by the gravitational dragging of the reference frame, but the issue is still not clarified. However, energy extraction from black holes via Poynting flux appears to be a very promising solution that overcomes the problems related to the transparency of the deep cores of AGNs to relativistic matter.

3.3 *Nonlinear Ejection Models*

Analytical solutions for the acceleration of jets from disks and magnetospheres around black holes are limited in their applicability. A time-dependent three-dimensional (3-D) analysis is required to explore the onset and evolution of the physical effects beyond the linear level. For this we can use numerical simulations, taking into account that numerical solutions are a valid approximation of the exact solutions, provided conditions of resolution, stability, and accuracy of the discrete integration domain are fulfilled. In general, these conditions are not known a priori, so testing and verification procedures are an essential part of modeling.

The equations of compressible fluid dynamics are coupled nonlinear, multidimensional, partial differential equations. They are transformed into a linear system of equations by a finite difference scheme and solved by adopting implicit or explicit algorithms with appropriate choices of grids. The treatment of dissipation terms governing the formation of shocks and discontinuities is the crucial point. Classical methods (e.g. Lax-Wendroff) were based on adopting dissipation terms in linear approximation (artificial viscosity) so that the

same amount is applied to all grid points. In hybrid methods (e.g. flux-corrected transport, FCT), numerical dissipation is nonlinear, as a high-order, more dissipative approximation is used in smooth regions of the flow and a low-order, less dissipative approximation near discontinuities. The most robust method for treating shocks is the Godunov method, adopted for instance in the Parabolic Piecewise Method (PPM) code, based on an upwind differentiation in the direction of characteristics; cells are considered to be uniform states, and a standard Riemann problem for the nonlinear waves is solved across the interfaces. A different algorithm is used in Smoothed Particle Hydrodynamics (SPH), based on treating cells as particles interacting via collisional terms.

Fluid simulations of accretion disks and supersonic jets are rather cumbersome because large integration domains are necessary to test whether evolutionary patterns are transient or correspond to stationary configurations before they hit the domain boundaries. This limits the number of spatial dimensions that can be used; only massive supercomputers allow fully 3-D simulations. More often, computations are done in 2-D or 2.5-D dimensions (including the third coordinate for vector components but in 2-D symmetry) and therefore completely miss nonaxisymmetric modes that are known to be important.

Finally, hydrodynamic models are simpler than MHD models, but the origin of acceleration goes back to ad hoc mechanisms such as radiation or thermal pressure. Maxwell equations increase the number of characteristics in the fluid system and make the numerical solutions more unstable. On the other hand, magnetic fields are essential in disk/jet modeling, and their correct representation is extremely important. In the following section, we discuss only MHD simulations, even though the existing numerical codes still have limited accuracy.

SWEEPING MAGNETIC TWIST The first attempt to study the time-dependent nonlinear magnetic disk/jet structure evolution was made by Uchida & Shibata (Uchida & Shibata 1985, Shibata & Uchida 1986), who solved an initial value problem in axisymmetric geometry using a Lax-Wendroff numerical scheme. More recently, these results have been extended to the complete 3-D geometry (Shibata & Uchida 1990) and to general relativistic conditions (Koide et al 1998). They assumed the existence of a geometrically cold thin disk with $(v_s/v_K)^2 \leq 10^{-2}$ rotating around a point mass at Keplerian or sub-Keplerian azimuthal velocities ($v_\phi/v_K = 0.6$–1.0), and they used ideal MHD equations in cylindrical geometry (r, ϕ, z). In their model, a uniform magnetic field such that $(v_A/v_K)^2 = 10^{-2}$–10^{-3} penetrates the disk vertically, and a nonrotating corona is present outside the disk. The rotating disk bends the poloidal magnetic lines and develops a toroidal structure. The buildup of magnetic tension in the disk is released along the poloidal lines as large-amplitude torsional Alfvèn waves (sweeping magnetic twist). This process extracts angular momentum

from the disk that starts collapsing toward the center: When the toroidal field has become strong enough, mass is ejected along the poloidal lines and gives rise to a hollow jet structure. The acceleration of the jet matter is essentially due to the $\mathbf{J} \times \mathbf{B}$ and centrifugal forces. The final magnetic configuration has a poloidal field in the form of an hourglass with a helical toroidal annulus moving axially at the local Alfvèn speed. In the jet, this local speed becomes greater than the Keplerian velocity; thus ejection velocities are a few times v_K. In the general relativistic version of the model, a fast flow, close to the rotation axis and confined by the hollow slow flow, is accelerated up to $v_j \sim 0.9$ c or $\gamma_j \sim 2$. The process applies to both Keplerian and sub-Keplerian disks, but the latter evolve faster and give rise to more vigorous jets. Near the disk the collimation of the jet is due to the poloidal field, while farther out the toroidal field pinches the outflow in the axial direction.

The Uchida & Shibata model deals with the disk in a fully dynamical way, including the response of the disk to the ejection of jets. However, the link between the two components is related to the mechanism of "numerical" magnetic field reconnection in the inner part of the disk, from where toroidal magnetic flux is ejected along poloidal field lines. The Lax-Wendroff scheme is highly dissipative and does not allow excessive enhancements of the toroidal field that could lead to disruption of the configuration.

Stone et al (1994), using a PPM code, extended the above results to the low magnetic field regime. In this regime, the dynamo process enhancing the disk magnetic field corresponds to the Balbus & Hawley's (1991) magneto-rotational instability. In fact, generation of enhanced accretion onto the central black hole can be observed as a result of the extraction of angular momentum by the Alfvèn torsional waves that arise from the instability.

More recently, the back-reaction of the jet formation has been studied by Matsumoto et al (1996) by referring to geometrically thick disks in axisymmetric conditions. Their results are very similar to those obtained for thin disks, but here the accretion avalanche can actually be seen to occur at the surface of the disks where torsional Alfvèn waves accelerate jets and remove angular momentum. Again, a crucial point is the detailed dynamical behavior at the inner edge of the disk. The accretion flows pulling the magnetic field from the upper and lower surfaces of the disk meet at the tip of the disk with opposite magnetic polarities. Magnetic reconnection may take place and may be used to produce nonthermal particles (see Section 6).

Whether the sweeping twist mechanism can reach a stationary configuration remains an open question. A condition for stationary inflow/outflow is the continuous supply of matter and magnetic field to the disk corresponding to the steady output of power along the jet by the Poynting flux of the torsional Alfvèn waves.

STATIONARY OUTFLOWS Romanova et al (1997) aimed to find stationary solutions. They assumed that an outflow originates from a disk that is considered as a fixed boundary condition; the initial magnetic field is taken to be a tapered monopole field. Matter is pushed out of the accretion disk with a velocity that is less than the slow magnetosonic velocity. It is then accelerated through the three MHD critical points and reaches a super-fast magnetosonic final velocity. Acceleration occurs especially in the innermost part of the system where the magnetic field is strong. These solutions do not show collimation at large distances, as the kinetic energy density prevails over the magnetic one. In contrast, according to Ustyugova et al (1995), stationary solutions are not possible for $\beta = v_s^2/v_A^2 \gg 1$. In that limit, the rotation of the disk generates a strong toroidal field that pinches the outflow, as in the sweeping twist.

Ouyed & Pudritz (1997a) have presented 2.5-D time-dependent simulations of the evolution of nonrelativistic outflows from Keplerian disks steadily orbiting a central point mass that is accreting at sub-Eddington rates. They used an extended version of the ZEUS-2D code (see next section). The disk is treated as a fixed boundary with a cold corona in stable equilibrium that is supported by Alfvènic turbulent pressure, most likely generated by the Balbus-Hawley instability (Balbus & Hawley 1991). The initial magnetic field configuration in the corona is a poloidal potential field ($\mathbf{J} = 0$), smoothly connected with a toroidal magnetic field in the disk that scales as $B_\phi \propto 1/r$. Gas is injected from the disk at very low speed into the corona ($v_z = 10^{-3} v_K$), where magnetic lines are opened to more than the critical angle for centrifugal acceleration through the Alfvèn and fast magnetosonic points and collimation in cylindrical structures parallel to the rotation axis. This collimation is due to the pinching force of the toroidal field that is self-consistently generated by the outflow dynamics (currents flow primarily along the axis); these results agree with the Heyvaerts & Norman's (1989) asymptotic analytic solutions. Stationary solutions are found for the adopted set of model parameters, in particular for relatively strong magnetic fields, with $\beta = 1$ at the innermost radius of the disk. The jet axial velocity v_z is a few times the Keplerian velocity at the fast magnetosonic point and then increases $\propto z$, as is expected theoretically from hydrodynamic models (Raga & Kofman 1992). A large fraction of the energy in the jet is in the poloidal kinetic energy (two thirds of the total), the rest in toroidal magnetic energy.

Meier et al (1997) have performed an extended analysis of the parameters space of time-dependent numerical simulations of the outflow induced by the corona of magnetized accretion disks, starting from axisymmetric configurations that are consistent with the Blandford & Payne analytical model. The strength of the magnetic field used in their simulations can be much higher than in most other simulations. They assumed a thin cold dense disk with a tenuous hot corona (but with temperature less than the virial halo that permeates the

system); initially, magnetic field lines are purely poloidal ($B_\phi = 0$) and are anchored in the disk and protrude into the corona at an angle $\theta \leq 60^\circ$ with respect to the disk. The resulting outflow is collimated into a jet in all cases, but its dynamical characteristics depend on the ratio $\nu = v_A/v_{esc}$, where v_A is the Alfvèn velocity in the corona and $v_{esc} = (2GM_h/R)^{1/2}$ the escape velocity. For $\nu \leq 1$, gravitational forces dominate over magnetic forces, and the jet is accelerated by an upward recoil due to an increase of the disk magnetic field by differential rotation. This acceleration has low efficiency and the final velocities are below v_{esc}. For $\nu \geq 1$, the jet is produced by magneto-centrifugal acceleration and is collimated by an azimuthal field; the final velocities are typically $v_j \geq 10 v_{esc}$ for v_A of the order of the Keplerian velocity at the inner radius of the disk and increase further for increasing v_A. The transition between the two modes of jets is rather sharp, and the authors use the term "magnetic switch": For small fields, the jet transports essentially magnetic energy in the advected magnetic field, and for large fields, the jet carries a significant amount of kinetic energy. The transferred energy does not show any switch in total power, and in either form, it is available for particle acceleration and radiation. Figure 4 shows the

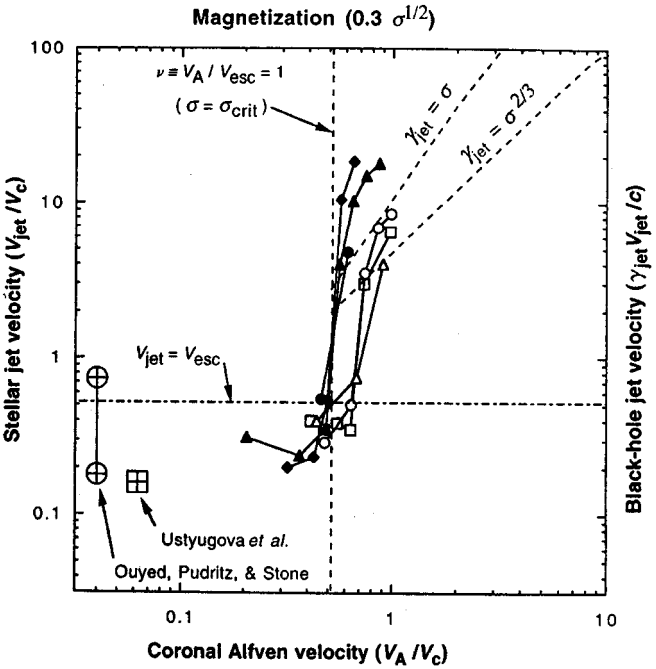

Figure 4 Numerical jet simulations from Meier et al (1997).

jet speed as a function of the coronal field strength and also includes results from simulations by other authors.

Meier et al (1997) suggest a possible correlation of weakly magnetized outflows with FR I jets and of highly magnetized ones with FR II jets. Their simulations are easily extended to the special relativistic case and show that current wind theories break down for low magnetic fields, as, in this regime, gravitational effects that are generally neglected become important. The bulk Lorentz factor of highly magnetized solutions can be as large as $\gamma_j \approx 10$.

EPISODIC OUTBURSTS Observations show that the brightness distribution in jets is very knotty, beginning at VLBI scales. In addition, short time-scale variabilities in blazars may be due to irregularities in the associated jets. Therefore, nonstationary outflow solutions are also interesting for modeling extragalactic jets.

Ouyed & Pudritz (1997b) applied their model to analyze the influence of the magnetic topology on the solutions and in fact have solved the case of bursting outflows. From the original Blandford & Payne analytic solution, it was clear that centrifugally driven winds are not possible if the poloidal magnetic lines are not open to an angle $\leq 60^\circ$ to the disk. Therefore, in a configuration where the initial lines are parallel to the rotation axis, the formation of winds is not expected. In reality, the progressive winding of magnetic lines in the disk generates large-amplitude nonlinear torsional Alfvèn waves, as in Uchida & Shibata's model. While the twisting of magnetic lines increases approaching the central parts of the disk, the ensuing strong gradient generated in the toroidal magnetic field opens up any vertically uniform magnetic structure. In particular for a hot corona $\beta = (v_s/v_A)^2 \sim 1$, a jet can be launched from the inner portion of the disk surface, where the magnetic lines are dragged equatorially toward the central object and the inclination angle to the disk becomes $\leq 60^\circ$.

However, the wind does not reach a stationary state because the strong toroidal field in a well-defined region of the inner jet tends to recollimate the flow toward the axis, producing MHD shocks. In this way, a compact confined structure is launched from the disk along the poloidal field; the process can repeat periodically. Knots would then be produced automatically in magnetic topologies aligned to the rotation axis, without invoking irregularities in the accretion flow or other exotic scenarios. However, it must be remembered that in these simulations, the disk is assumed to be a fixed boundary and back-reaction effects are neglected.

Contopoulos (1995) has proposed another possible scenario for episodic outburst that we commented on above. He assumed that no poloidal field is present in the corona, only a toroidal component in the disk. The strong pressure gradient between the disk (B_ϕ large) and the corona above it ($B_\phi \simeq 0$) forces

plasma out perpendicularly to the disk. The explosively ejected plasma convects azimuthal magnetic field and is self-collimated. Contopoulos presented a simple time-dependent analysis of the process, showing that plasma is unstable to pinch instabilities that confine sheets of radial currents in the jets.

3.4 *Observable Quantities*

POWER In the Blandford & Payne model, the ratio of jet and disk luminosities is

$$\frac{\dot{m}_j}{\dot{m}_d} \sim \epsilon \ln (r_{0\,\max}/r_{0\,\min}) , \tag{10}$$

where $r_{0\,\max}$ and $r_{0\,\min}$ are the outer and inner disk radii and ϵ is an efficiency factor of transformation of binding energy at $r_{0\,\min}$ into jet power. For the estimated parameters, this ratio is always $\ll 1$; i.e. only a small fraction of the accreted mass has to go into the wind. Only for relatively high-mass discharge onto the jet, $\dot{m}_j \sim 0.1\ M_\odot$/year $\sim 0.1\,\dot{m}_d$, can the power in the jet reach $L_j \sim 10^{46}$ erg s^{-1}; this makes it difficult to explain the energetics of strong sources (see Section 2), especially when taking into account that only a small fraction can be transformed into radiation. Analytic results are confirmed substantially by the numerical simulations we discussed above. Hydromagnetic jets appear to be a very efficient way to extract energy from accretion disks, but perhaps a relativistic treatment is needed to fit the parameters well.

In this respect, unipolar inductor–type models are more promising. Camenzind (1998) showed that the Poynting flux of a rotating axisymmetric Kerr black hole magnetosphere can carry a magnetic luminosity:

$$L_{mag} = \frac{1}{c}\Omega_h I_h \Psi_h \simeq 3 \times 10^{46} \left(\frac{M_h}{10^9\ M_\odot}\right)^{-1} \frac{\Psi_h}{10^{33}\,\mathrm{G\ cm^2}} \frac{I_h}{10^{18}\,\mathrm{Amp}} \mathrm{erg\ s^{-1}}, \tag{11}$$

where Ω_h is the rotational velocity at the Kerr horizon and I_h the total current and Ψ_h the magnetic flux, respectively, integrated over the horizon.

While the understanding of the jet dynamics has progressed substantially, the problem of powering jets and enabling them to emit nonthermal radiation with luminosities up to $\sim 10^{47}$ erg s^{-1} is still far from being solved.

ASYMPTOTIC BULK VELOCITY In most jets, asymptotic bulk velocity is estimated indirectly through proper motions at VLBI resolution or through advancement velocities of extended structures or required Doppler beaming. This bulk velocity has to be supersonic and, in the inner portion of jets, relativistic, with Lorentz factors up to $\gamma_{bulk} \sim 20$. In general, the asymptotic velocity of outflows in hydromagnetic models is a few times the Keplerian velocity at the

base of the flow, which corresponds to super-Alfvènic and relativistic velocities and allows Lorentz factors that are as large as needed, $\gamma_{bulk} \sim 10$–20. Kudoh & Shibata (1995) have investigated 1.5-D steady MHD winds from accretion disks, including thermal effects, and they obtained a relation between the jet mass flux and the magnetic energy of the disk. Their calculations confirm the above results for the terminal velocity with a weak dependence on the magnetic energy of the disk, $v_\infty \propto B^{1/3}$.

4. JET CONFINEMENT: THE INTERACTION WITH THE AMBIENT MEDIUM

Observations show that an AGN jet undergoes a huge expansion at the exit from the inner core. In a few parsecs, its radius multiplies by a thousand or more. Afterwards it recollimates to a conical structure with a small opening angle, without apparently going through any dramatic event, and travels megaparsec distances while maintaining its directionality. Instead, laboratory experiments with fluids indicate that both dense and light flows (with respect to the external medium) expand at the sonic speed and suffer various types of fluid instabilities, developing vortices and internal shocks. After a few scale lengths, collimation is lost, velocities become subsonic, and flows are disrupted (van Dyke 1982). For light jets, disruption is due primarily to matter entrainment and mixing, and for dense jets, to thermal expansion.

This morphological difference initially prompted the idea that extragalactic jets were highly supersonic, freely expanding flows in underdense atmospheres with a negative density gradient. As shown in laboratory experiments (Thompson 1972), after exiting the nozzle, the flow expands with a bending of streamlines fixed by the local Mach number M_j; for $M_j \gg 1$, the opening angle $\theta \approx (M_j)^{-1}$. On the other hand, the jet radial evolution emerging from high-resolution observations is much more complex than expected in freely expanding jets. Jets must be confined, but at the same time the interaction with the external gas is nondestructive. Incidentally, we mention that "ballistic confinement" of a stream of dense aligned bullets has been discarded on the basis of global energetics, as it would require kinetic luminosities that are too large and would imply fast deceleration (Pacholczyk 1977).

"Thermal pressure confinement" by interstellar and intergalactic matter is the most natural possibility, as already mentioned in the Introduction. Minimum jet pressure is estimated from the equipartition argument in the synchrotron model, while external thermal pressures can be evaluated from X-ray observations. As discussed by Feretti et al (1995), internal pressure in FR I jets is below external pressure. The situation is more complicated for FR II powerful jets. For instance, knots and filaments in the jet of M 87 are out of pressure equilibrium

and overpressured by a factor of $\sim$10 with respect to the external medium, although these may simply be transient structures, given the relatively short lifetime of this jet (Bicknell & Begelman 1996). Also, the projection effect and filling factor may affect the estimates of internal pressure when applying the equipartition argument to jets that point to the observer. Finally, pressure confinement models require a well-tuned external pressure profile to maintain small opening angles over several decades of length scales. A related possibility is "inertial confinement" by a cold ambient medium, in which ram pressure is used to oppose jet expansion (Icke et al 1991).

External magnetic field confinement can be provided by a large-scale intergalactic field frozen in the inflowing plasma. This field corresponds to the poloidal fields assumed in all MHD models of jet acceleration from disks: The plasma collapsing into the central black hole deforms the fields into an hourglass shape that reaches an asymptotic cylindrical geometry outside the core (Heyvaerts & Norman 1989). However, laboratory plasma experiments do not allow much confidence in the stability of this field structure. A virial theorem argument shows they are highly unstable with regard to interchange and diffusion.

A more satisfactory approach seems to be self-confinement by internal magnetic fields. As noted in the previous section, pinching toroidal magnetic fields are consistently generated by differential rotation of the disk at the base of the jet and advected along the rotation axis. We discuss below how a backflow is formed at the working surface, where the advancing supersonic head impinges upon the confining medium. A shear layer is formed around the jet where instabilities and turbulent field amplification and/or dissipation play a major role in the dynamics, leading to mass entrainment and mixing (De Young 1996). A magnetized overpressured region around the jet is then formed that may in fact be the real confining agent.

4.1 *Global Dynamics of Confined Jets*

The propagation of a laminar jet confined by external agents in stationary hydrodynamic conditions is governed by the mass and momentum conservation laws. In the Newtonian, nonrelativistic limit and for a polytropic gas $P = K\rho^{\delta}$,

$$\rho v A = \dot{m}_j \Rightarrow P^{(\delta+1)/2\delta} M_j A = \text{const}; \tag{12}$$

$$P^{(\delta-1)/\delta}\left[\frac{M_j^2}{2} + \frac{\delta/\Gamma}{\delta-1} + \frac{\Phi}{c_s^2}\right] = \text{const}, \tag{13}$$

where M_j is the flow Mach number, Φ the gravitational potential, Γ the adiabatic index of the gas, and $\dot{m}_j$ the mass discharge. Equations 12 and 13 can be solved in the limit of given jet power and discharge $\dot{m}_j$. The cross-sectional area

typically shows a minimum value for $P_{\min} \sim (1/2)P_0$ (P_0 is the speed at the base of the flow, the stagnation point), where the jet speed becomes transonic. An adiabatic jet accelerates to supersonic speed passing through a converging nozzle. In the subsonic part of the flow, pressure and density are approximately constant, and $A \propto v^{-1}$ (Blandford & Rees 1974).

For the large-scale hypersonic part of the flow, $M_j \gg 1$, Equations 12 and 13 give $M_j \propto P^{(1-\delta)/2\delta}$ and $A \propto P^{-1/\delta}$, implying $v = \text{const}$; for an adiabatic flow $\delta = 5/3$, the scaling is $M_j \propto P^{-4/5}A^{-1}$, $A \propto P^{-3/5}$. Pressure distribution in galaxies can be modeled as $P_{ext} \propto r^{-n}$ (here r is the distance from the core), and the angle subtended by the jet width as seen from the nucleus decreases as $\theta \sim A^{1/2}r^{-1} \propto r^{(n-2\delta)/2\delta}$. For an adiabatic flow in a halo with $n = 2$, the opening angle is $\theta \sim r^{-2/5}$. Therefore steady jets can be collimated even though their area expands. On the other hand, the estimated equipartition pressure inside a jet scales as $P \propto A^{-2/7}$, i.e. falls much less rapidly than the equilibrium solution $P \propto A^{-5/3}$. This means that some form of internal dissipation must favor collimation.

A more complete analysis of the global dynamics of jets that takes into account confinement in channels, nonthermal momentum deposition or subtraction by external fields (radiation, plasma waves, etc) and in extended gravitational potential wells has been developed in compressible hydrodynamics by Ferrari et al (1985). They discussed quasi–2-D solutions of the problem of relativistic equilibrium flows for given profiles of the propagation channels, obtaining an equation for the flow velocity along the rotation axis:

$$\gamma^2 \left(1 - \frac{\beta_s^2}{\beta^2}\right) \frac{dB^2}{dZ} = -\frac{B}{Z^2} + \frac{2\beta_s^2}{S}\frac{dS}{dZ} + \frac{2D(Z)z_0}{\gamma^2 \rho c^2}, \tag{14}$$

where

$$Z = \frac{z}{z_0}, B = \frac{2GM}{z_0 c}, S(Z) = \frac{A(Z)}{A(z_0)}, \beta_s = \frac{v_s}{c}. \tag{15}$$

The first term on the right-hand side is the gravitational term. The second is very interesting: It easily can be derived that when the channel $S(Z)$ expands more (less) rapidly than spherically ($\propto Z^2$), its walls will deposit (subtract) momentum. The last term indicates momentum addition by external forces; for the case of radiation in the limit of optically thin plasma,

$$D(Z) = \frac{GM\rho\gamma^3 L}{z_0^2}[H(1+\beta^2) - \beta(J+K)], \tag{16}$$

where H, J, and K are the momenta of the radiation field.

Relativistic flows from accretion funnels exhibit many critical points, as compared with the single critical point (de Laval nozzle) of the nonrelativistic

hydrodynamic wind solution. In particular, the sudden expansion at the exit of the funnel brings the first critical point close inside the nucleus. In these solutions, the thrust is not constant, decreases in the subsonic regime, and increases in the supersonic regime. In fact, the surface of the jet is not parallel to the flow, and this corresponds to an external pressure force acting consistently on the field: Where the channel narrows (widens), the flow is slowed down (accelerated).

Steady Newtonian and relativistic solutions show that variations in the channel cross section due to the physics of external confinement act exactly like momentum deposition. Additional critical points of complex mathematical topologies produce jets with several transitions from a subsonic to supersonic regime through shocks. The production of shocks is very interesting in connection with the observations of extended jets with bright knots, as they provide suprathermal particle acceleration and field compression that locally enhance nonthermal emission (see Section 6). In addition, the flow pattern depends on the profile of the extended gravitational potential outside the nucleus. In particular for adiabatic jets, a mass distribution $M_{gal} \propto r^{-s}$, with $s \leq \delta$, does not allow the flow to reach a transonic point: The flow is stopped inside the galaxy (Ferrari et al 1986).

4.2 *Global Electrodynamics of Confined Jets*

The basic assumption in magnetic confinement of large-scale jets is that magnetic flux is advected by the flow that originates from accretion disks, although more flux can be added by entrainment of external magnetized matter or by internal stresses. From the solutions of the previous section, both poloidal B_p and toroidal B_ϕ magnetic components are supported by the dynamics of accretion disks and extend to large scales. A poloidal component actually increases internal jet pressure and loosens collimation, while the toroidal component pinches the flow toward the axis, although it may then favor instabilities. In an expanding jet, magnetic fields are expected to decay owing to expansion, as $B_p \propto R^{-2}$ and $B_\phi \propto R^{-1}$, where R is the jet radius. This behavior agrees qualitatively with typical observations showing the initial part of the jet dominated by longitudinal (poloidal) fields and later by the perpendicular (toroidal) component. On the other hand, synchrotron luminosity does not decay as rapidly as the simple adiabatic expansion law would predict, $L \propto R^{-(5+4\alpha)}$ (α spectral index). Thus, magnetic flux must be added along the flow, most likely through entrainment, turbulent shear amplification, or dynamo effects (De Young 1980).

An analytic study of the structure of magnetized jets outside the acceleration and collimation zone is performed by looking for solutions of the asymptotic MHD wind equations. The classical self-similar solution by Heyvaerts & Norman (1989) shows that jets after the acceleration phase are recollimated

by the toroidal field generated by the disk rotation and become cylindrically confined. Chiueh et al (1991) extended the study to relativistic flow speeds, showing that flux surfaces either collimate to current-carrying cylinders or to current-free paraboloids. Similarly, Lovelace et al (1987) showed that, by including a rotating force-free magnetosphere outside a Keplerian disk, jets can be self-pinched.

The confinement of the flow is governed by the Grad-Shafranov equation (Appl & Camenzind 1993a), in which currents and current gradients are essential in the structure of jets. While collective effects in plasmas are very efficient in maintaining charge neutrality, jets may carry a net current, especially when considering a plasma with both thermal and suprathermal relativistic components (Sol et al 1989). The idea of self-confinement by the tension of toroidal field lines in current-carrying jets was originally proposed by Benford (1978). He showed that the total net current involved in an axisymmetric jet solution is $I \sim 10^{17} P_{-12}^{1/2} d_{kpc}$ Amp in typical units (P is the pressure). Confinement can be achieved by a radial field profile $B_\phi \propto 1/R$ so that magnetic stresses reach equilibrium with the external medium at some radius.

Appl & Camenzind (1993a,b) discussed force-free relativistic magnetized jets in terms of the radial distribution of poloidal current $I(R) = cRB_\phi/2$. They solved the Grad-Shafranov equation for given current distributions, which can take into account variations of the jet radius. Equilibrium solutions are found for jets with a current-carrying core [$R_c = \gamma\,(v/c)\,R_L$, where R_L is the light cylinder radius] enveloped in a current-free envelope. The jet core is electromagnetically dominated, as the Poynting flux is concentrated on the jet axis. In dense regions close to the AGN core, the shape of the jet is determined by the ambient pressure. Any amount of current inside the jet is compensated by a return current on the jet surface. Once the ambient pressure drops below the electromagnetic pressure on the jet, boundary self-confinement begins and the shape of the jet becomes cylindrical. Various current radial distributions have been studied, and in a cylindrical force-free jet, it has been proven that only part of the current and return current can flow inside the beam.

Other studies of magnetic self-confinement refer to fields generated by surface currents at the interface between the jet and a surrounding cocoon (Cohn 1983). Others focus on helical equilibria, although without a consistent explanation of the origin of ordered longitudinal fields that are linked to predefined boundary conditions (Chan & Henriksen 1980, Villata & Ferrari 1995, Trussoni et al 1996).

4.3 *Jet Instabilities*

In their original proposal that extended radio galaxies are continuously powered by supersonic, relativistic outflows from galactic nuclei, Blandford & Rees (1974) pointed out that laboratory experiments (mostly subsonic) show

that collimated beams maintain their directionality for relatively short distances (typically less than 10 times their diameter) owing to onset of fluid instabilities, shocks, boundary layer effects, and turbulent mixing with the external medium (Brown & Roshko 1974). Astrophysical supersonic and/or super-Alfvènic jets appear instead to be much longer lived, although they are modulated by knots, bends, and internal shocks of the same type observed in the laboratory. Therefore, several calculations have since been addressed to the question of pressure-confined jet stability (Blandford & Pringle 1976, Turland & Scheuer 1976, Ferrari et al 1978). In this section, we address jet stability against perturbations at the boundary layers with the confining medium created in the collimation zone, without considering perturbations coming from the flow's "head."

LINEAR KELVIN-HELMHOLTZ INSTABILITY In the case of pressure-confined fluid beams in relative motion with respect to an external medium, the typical instability is the Kelvin-Helmholtz instability. If a ripple develops at the interface between the two fluids in relative motion, the flow over the ripple has to be faster and, therefore, according to the Bernoulli equation, exerts less pressure and allows the ripple to grow further. This causes mixing of the two fluids and transfer of momentum across the boundary, with a progressive destruction of collimation and slowing down of the flow (Chandrasekhar 1961, Gerwin 1968).

In our astrophysical context, this instability has been studied for supersonic, compressible, relativistic pressure-confined jets in cylindrical, slab, or conical geometries, both for axisymmetric and nonaxisymmetric perturbations, with and without a magnetic field, and with rotation; for a review, see Birkinshaw (1991). The linear stability analysis is based on perturbing the equilibrium shear layer between the two fluids with small-amplitude Fourier modes $\propto \exp[-i(\omega t - \mathbf{k}\cdot\mathbf{r})]$ and linearizing the perturbed equations with matched boundary conditions across the shear. The resulting (algebraic) dispersion relation $D(\omega, \mathbf{k}) = 0$ is then studied to find modes with Im $\omega > 0$ (locally growing modes) or Im $k < 0$ (spatially growing modes). When such modes exist, the equilibrium of the fluid can be destroyed, unless saturation effects stop the growth of the perturbations in the nonlinear regime. A systematic method to explore the complete stability diagram is presented by Bodo et al (1989).

Two types of modes exist in jets: ordinary surface modes, with amplitude steeply decreasing away from the interface, and reflected body modes, which affect the whole plasma in the jet. Body modes are typical of supersonic jets. While ordinary modes are already unstable in single-shear problems, reflected modes are stable in single shears but become resonantly unstable by reflections in a two-shear configuration, such as slabs or cylinders (Miles 1957). Their velocity with respect to the fluids is typically $\sim \pm v_{rel}/2$, half of their relative velocity. Resonant reflected modes have propagation wave vectors inclined by

an angle $\sim 1/M_j$ over the shear surface. The most unstable wavelengths are typically

$$\lambda_{KH} \sim 2\pi R M_j, \tag{17}$$

with temporal growth times

$$\tau_{KH} \sim \frac{1}{\mathrm{Im}\omega} \sim \kappa \frac{\lambda_{KH}}{R} \frac{2R}{c_s}, \tag{18}$$

where R is the beam transverse scale and $\kappa \leq 0.5$ a factor depending on the specific geometry, mode, and density contrast; for magnetized beams, c_s is replaced by c_A. Ordinary modes dominate for $M_j \leq 2\sqrt{2}$, and reflected modes above this limit. High density in the jet and strong magnetic fields reduce the effect of instability. In particular, the presence of magnetic fields, both longitudinal and transverse, has a stabilizing effect but mainly on small-wavelength modes. Thus, the development of turbulence and dissipation is avoided, and strongly magnetized jets can be considered substantially laminar. However, long-wavelength modes take over, though less rapidly, and may develop into strong modulation of the flow. Modes are completely stabilized for $c_A/c_s \geq 2$.

A critical element in the instability evolution is the physical extent of the contact layer between the jet and the ambient medium. At the origin of jets, the so-called vortex sheet approximation, with steep velocity and density gradients across the layer, can be adopted, but after some distance, it may be more appropriate to use an extended transition zone that is created by matter entrainment and other nonlinear effects. Then all modes with wavelength shorter than the gradient scale are stabilized.

Instability time scales are rather short with respect to the propagation time scale, and therefore these modes can affect AGN jets soon after the exit from the nozzle. Long-wavelength modes modulate the morphology of the beam, while short wavelengths can give rise to a turbulent cascade that eventually leads to thermal dissipation and suprathermal particle acceleration.

In current-carrying jets, current-driven instabilities also must be considered. However, Appl & Camenzind (1992) have shown that their growth rates are always below that of Kelvin-Helmholtz modes.

Finally, we mention that rotation around the jet axis tends to stabilize ordinary modes at all wavelengths for low M_js and at small wavelengths for large M_js. This makes the importance of reflected modes in rotating jets (Bodo et al 1996).

FILAMENTATION INSTABILITY Another type of intervening instability is the synchrotron "thermal" instability (Eilek & Caroff 1979, Bodo et al 1990). If the pressure in jets is mainly due to the relativistic electron component, synchrotron losses in regions compressed by fluid instability start the runaway effect of thermal instabilities (Field 1965). The compressed gas will radiate

more and reduce the gas pressure, leading to further compression. In a situation out of equipartition, $\beta = P_{rel}/P_B \gtrsim 4$, condensation modes with $k_\parallel \ll k_\perp$ modulate the magnetic field into longitudinal filaments. These may be overpressured with respect to the external plasma and should appear brighter than the surrounding medium because of enhanced emission, provided a suitable input of fresh relativistic particles is guaranteed (Rossi et al 1993). These instabilities may be associated with the observations of radio and optical filaments in jets as M87 and 3C66B.

RESISTIVE INSTABILITIES Most important instabilities in magnetically confined jets are reconnection modes. They develop in magnetic neutral sheets or shears across which a component of the field is inverted. A thin dissipation layer is produced at this sheet in which flux freezing is violated and magnetic flux can be annihilated (Biskamp 1994). For a beam with a helicoidal field wrapped around cylindrical surfaces, the equilibrium conditions predict a field pitch angle that decreases away from the axis. When a nonaxisymmetric perturbation is excited along the beam, its pitch angle will match the equilibrium pitch angle at some well-defined radius $R_{crit} \propto B_\phi/B_\parallel$. That cylindrical surface becomes a neutral sheet for the component of the field vector perpendicular to the perturbation wave vector. The end result is field annihilation and local heating and/or particle acceleration. The growth rate of these modes is relatively slow, but indications of an explosive nonlinear phase have been obtained in laboratory experiments (Ferrari 1984).

In the same context, Blackman has discussed how slow-mode shocks are formed in reconnection regions around magnetic X-point topologies (Blackman 1996). These shocks correspond to lower magnetic flux downstream than upstream of the front. Consistently fast particle acceleration can take place in regions of low $\beta = P_{gas}/P_B$.

4.4 *Nonlinear Evolution of Jet Dynamics*

The numerical approach to the study of jet dynamics is an approximation of the real physical situations. In fact, although numerical simulations have become very sophisticated owing to supercomputers, nevertheless, the solution of the set of Navier-Stokes or Euler plus Maxwell equations is still limited to relatively low Reynolds numbers (high viscosity) $Re \leq 100$ owing to the discretization process by finite difference schemes. On the other hand, laboratory experiments indicate that for highly supersonic jets above these values of Re, the physics does not change appreciably from the phenomenological point of view.

HYDRODYNAMIC SIMULATIONS *Temporal analysis* Early simulations of the evolution of instabilities in cylindrical or slab symmetry were presented by Hardee & Norman (1988) but were rather limited in time. Bodo et al (1994, 1995) and Basset & Woodward (1995) have followed the evolution of unstable

modes in infinite 2.5-D cylindrical jets and 2-D slabs. By applying periodic boundary conditions at the initial and final cross sections of the jet at the extremes of the integration domain, they simulated the evolution of local perturbations of wavelengths shorter than the domain length in an infinite flow. This is called a temporal analysis of the instability. In this way, the instability can be followed to see whether nonlinear saturation effects yield to the onset of a quasistationary state. Bodo et al (1994), following an exploration of the relevant parameters, i.e. density contrast $\nu = \rho_{ext}/\rho_j$ and Mach number M_j, determined that jets, after a time $t \sim 30R_j/c_s$, reach a quasistationary highly turbulent configuration. Heavy jets maintain a coherent directionality; light jets appear completely mixed and diffused. In conclusion, the persistence of jets depends principally on the density contrast with the ambient medium. Examples of the evolution are illustrated in Figure 5*a*,*b*.

The situation changes drastically in 3-D simulations of cylindrical jets (Bodo et al 1998). Mixing starts much earlier owing to the more rapid growth of small-scale structures, and this is particularly evident in light jets, where fluting modes are present in the linear phase with growth rates that are already larger than those of helical modes. Light jets are asymptotically disrupted by a strong transition to turbulence. Dense jets survive as collimated structures, although the energy and momentum lost by entrainment is larger and the process occurs faster, over time scales of $t \sim 10R_j/c_s$. The final flow velocity also is reduced, and the jet cross section is broadened, as is consistent with strong mass entrainment, which can reach the same load of the jet mass (see Figure 5*c*).

The physical reason for the instability enhancement in 3-D geometry is the faster development of small-scale structures independently from the initial perturbation. These can be either excited directly, owing to the large growth rate of nonaxisymmetric 3-D modes, or indirectly, through the nonlinear turbulent cascade of energy from large- to small-scale eddies. Another effect that appears to be important in this respect is the different scaling of volumes that makes 3-D jets more expanded.

On the other hand, recent numerical results appear to confirm a result of linear calculations, which shows that the presence of an extended layer around the jet can stabilize the flow by suppressing perturbations with scales smaller than the transverse dimension of the layer. As we discuss in the next section, the formation of layers is admissible under the form of a cocoon produced by the bow shock of the advancing head of the jet or to nonlinear fluid effects at the flow boundary.

Spatial analysis In a different numerical approach, the flow is considered as a finite window on an infinite jet with free boundary conditions at the extremes of the integration domain, and perturbations are produced at the injection nozzle.

These perturbations are then followed in their spatial growth while crossing the integration domain and passing through a still undisturbed medium. In this way, nonlinear spatial effects can be analyzed as, for instance, the interaction and merging of shocks along the jet (Norman et al 1988, Micono et al 1998).

The nonlinear evolution of spatial axisymmetric perturbations in 2-D cylindrical and slab structures essentially agrees with the temporal analysis in its initial three stages. The axisymmetric perturbation that dominates eventually is the first reflected mode that actually has the fastest spatial growth rate. A tendency is observed of coalescence of successive shocks into an almost transverse single strong shock that extends into the external medium through entrainment and momentum dissipation.

Antisymmetric perturbations in cylindrical jets or nonaxisymmetric perturbations in slabs instead create piston-like protrusions (spurs) into the external medium that travel along the integration grid. They can never reach the quasi-stationary stage because the spur amplitude becomes very large while travelling along the jet and in fact disrupts the ordered flow (Norman et al 1988, Micono et al 1998). In addition, longitudinal filamentary structures develop that can wrap around the jet if rotation is included in the calculations (Hardee & Stone 1997).

Cooling jets A crucial question is whether radiative losses can affect the global evolution of the instability. In most 2-D cases, even when counteracted by heating, they slow down the growth of instability (Rossi et al 1997, Stone et al 1997, Micono et al 1998). In cylindrical geometry, thermal losses (a case that best applies to stellar jets) are very efficient in suppressing mixing of the jet matter with the external medium, and subsequently matter entrainment. Shocks remain well separated and maintain the characteristic zigzag pattern. However, mixing is present in dense jets. For a slab, mixing and shock coalescence develop on short time scales, and the growth of the instability may in fact be faster. In the case of synchrotron losses, which are more appropriate to extragalactic jets, in addition to Kelvin-Helmholtz–type instabilities, filamentation modes related to thermal-type instabilities are most important and modulate the jets longitudinally (Rossi et al 1993). In fully 3-D geometries that are characterized by faster growth of the instability, radiation losses appear to be too slow and unable to stop the disruption of jets.

MHD SIMULATIONS From a historical point of view, we recall that a 2-D MHD particle code was used by Tajima & Leboeuf (1980) to study Kelvin-Helmholtz instabilities of a single shear layer parallel to a uniform magnetic field but did not reach long time scales of evolution. The numerical analysis of nonlinear MHD instabilities is still limited to rather simple configurations. Most experiments performed so far have used the standard finite difference scheme

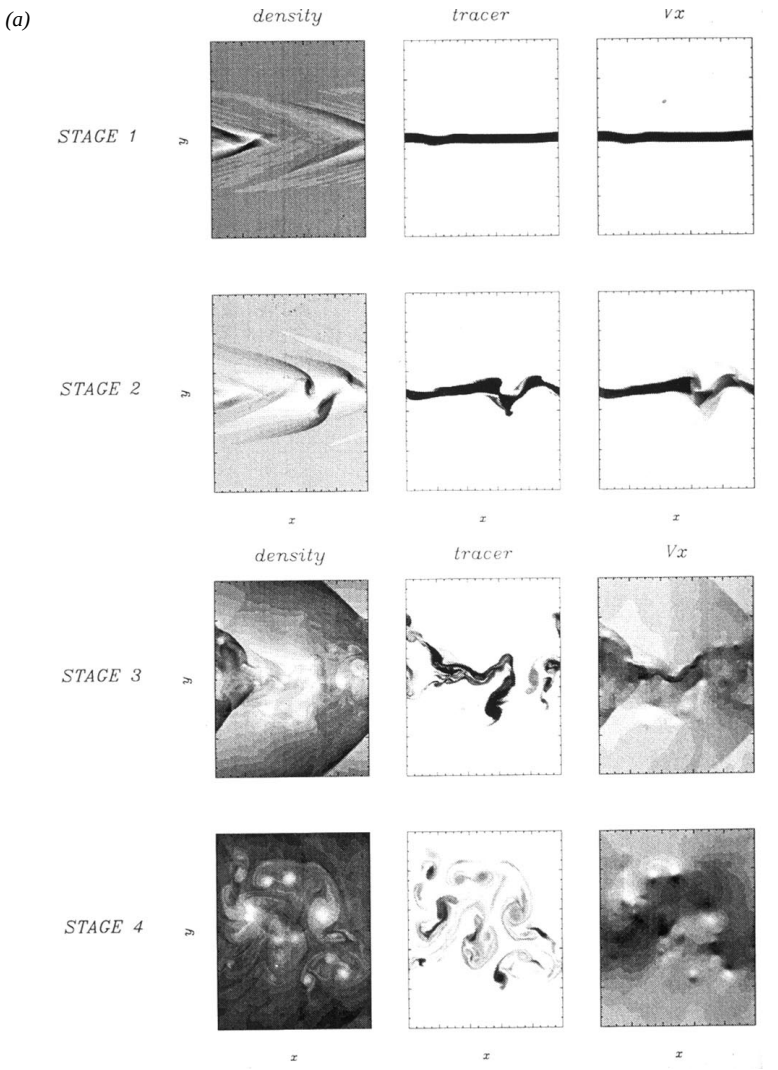

Figure 5 Long-term evolution of Kelvin-Helmholtz instabilities (Bodo et al 1994, 1995, 1998): (*a*) the four phases of evolution in a slab ($M = 5$, $\gamma = 1$); (*b*) the physical parameter space $M - v$ in a two-dimensional (2-D) cylindrical jet; (*c*) strong instability and turbulence in fully three-dimensional (3-D) jets.

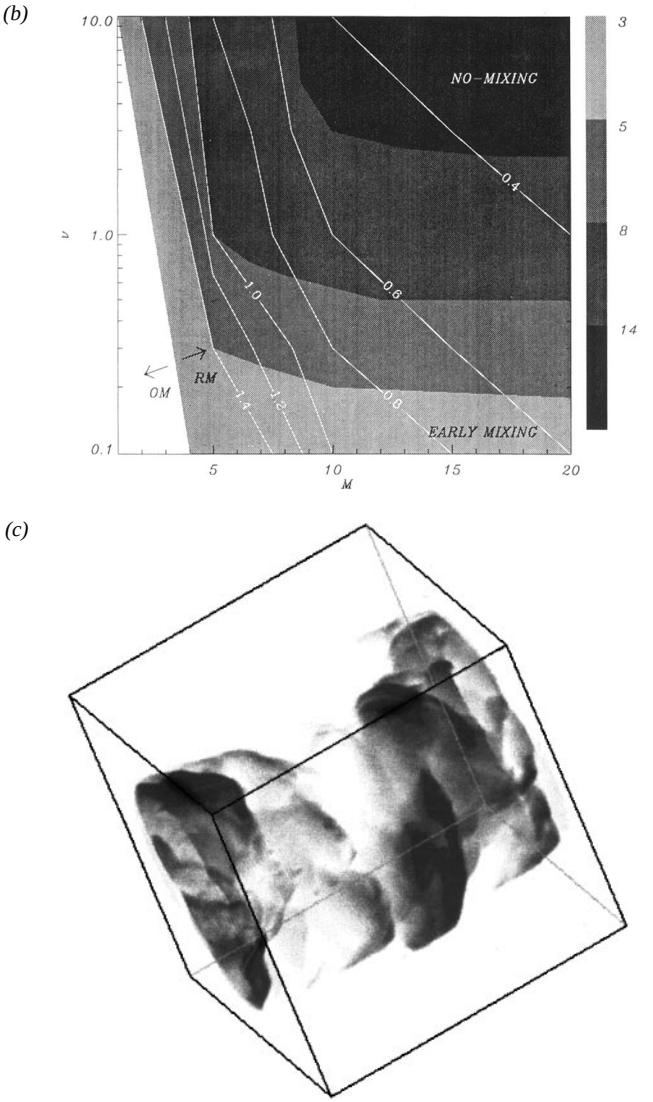

Figure 5 (*Continued*)

with finite cells and, correspondingly, a rather large numerical viscosity. Shibata & Uchida (1986) used an evolved Lax-Wendroff scheme. Stone, Norman, and collaborators (Stone & Norman 1992, 1994) developed a 2-D MHD code named ZEUS that is partly based on a higher-order upwind integration scheme. An extension of this last code to a 3-D case is now available but has low resolution for studying the formation of vortices and turbulence. As a consequence, these simulations tend to smooth out strong instabilities and discontinuities.

Recently, Zachary et al (1994) have succeeded in producing a 2-D MHD code with parabolic upwind integration along the characteristics across discontinuities. This MHD Godunov code has been tested on the standard problem of the Kelvin-Helmholtz instability of a shear layer in the case $c_A < c_s$ (large magnetic fields suppress the instability) (Malagoli et al 1996); the formation of cats' eyes has been followed, and the subsequent series of reconnection events asymptotically yields a stationary turbulent thick layer (Figure 6). A relatively

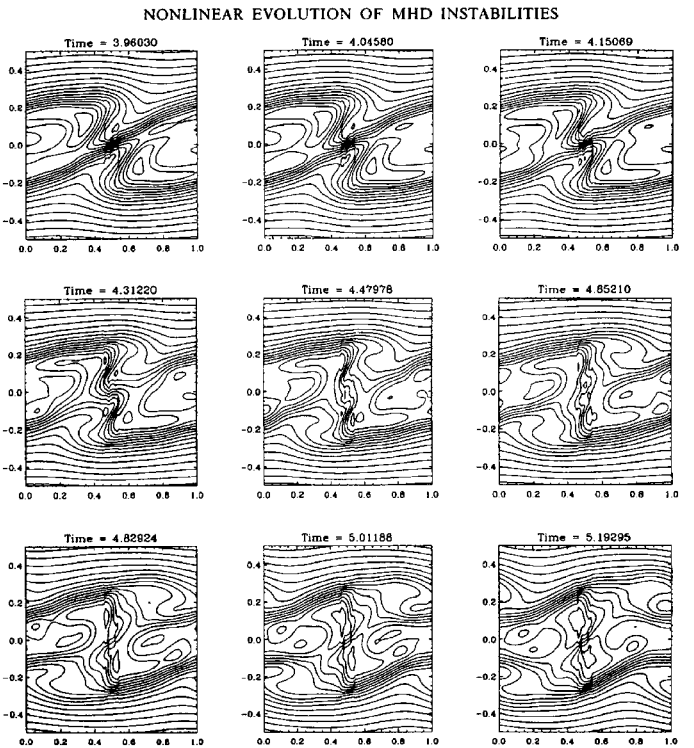

Figure 6 Numerical simulation of a reconnection event (Malagoli et al 1996).

small magnetic field, well below equipartition, helps the shear layer reach a stationary state in which the two fluids in relative motion are separated by a turbulent boundary sheath that eliminates direct interaction. Thus, reconnection seems to be the crucial physical process in governing the magnetic instability evolution. Similar results have been obtained by Frank et al (1996) and Min (1997) using an FCT code.

SHOCKS We conclude discussing in more detail the evolution of "internal shocks" already predicted in linear studies but now properly followed by numerical methods. These shocks arise in the form of conical structures inside a cylindrical jet with typical opening angles of $\sim 1/M_j$. The repetitive pattern of oblique shocks is a typical feature of the nonlinear evolution of jets. All these shocks travel with the flow at a velocity slightly below the jet velocity and may be related, as shown in Section 6, to emission morphologies. The intersection points of shocks correspond to high pressure regions with strong emission. Actually, as shown by Hardee & Norman (1989), the merging of shocks gives rise to phase effects where the intersection points can move at a velocity higher than the jet's. This is clearly relevant to the interpretation of superluminal motions in relativistic jets. In later stages, owing to mass entrainment and momentum diffusion, shocks extend at large distances into the external medium perpendicular to the flow and become substantial transverse structures (Bodo et al 1994).

4.5 *Astrophysical Applications and Comments*

The general conclusion from the above simulations is that shear instabilities are crucial in the propagation of supersonic jets. Nonlinear effects may stabilize magnetic and/or dense jets, but light hydrodynamic jets are prone to disruption by turbulent mixing on time scales that are short with respect to observed scales. Observations do in fact point toward the light jet case. The solution seems to be the reduction of the interaction between the jet and the external medium, either by magnetic fields or the presence of extended boundary layers or surface currents.

The application of the above results to classes of radio galaxies predicts that, if jets have similar initial M_j, FR I jets, which are turbulent and strongly decelerated, should correspond to dense environments (light jets), and FR II to lighter environments. The morphology of jets would depend on the ambient density, which is in agreement with a suggestion by De Young (1993). However, M_j may also have an influence. In particular, for a similar density ratio, highly supersonic jets tend to be less turbulent (FR II sources), and mildly supersonic jets more turbulent (FR I sources). These results fit in the unification schemes discussed in Section 2.2.

5. JET TERMINATION: THE COCOON

Jets terminate in extended radio lobes, where they release their energy and momentum into the ambient intergalactic medium through complex physical processes; see for instance the western radio lobe of Cygnus A for a typical example (Carilli et al 1996). A phenomenological analysis of the physics of this region is given below as a starting point for presenting the nonlinear models.

5.1 *Hot Spots*

Parker, in his model for solar wind, suggested that the supersonic solar wind solution must be connected to the subsonic dynamics of the interstellar medium through a "termination shock" matching the asymptotic wind to a breeze solution with $P_\infty \neq 0$ (Parker 1958). In laboratory experiments of collimated jets, this is accomplished through a strong planar shock, or "Mach disk," that creates a localized high pressure region. In extragalactic jets, this feature is identified with the hot spots, compact overpressured features, that are especially evident in FR II jets; they are instead dim or absent in weak FR I sources, most likely because strong turbulent dissipation in the propagation phase reduces the momentum finally released at the termination shock.

The location of the jet head, in particular that of the hot spots, is defined by balancing the internal thrust and external medium ram pressure:

$$\Pi_j \sim \frac{L_j}{(v_j - v_h)} \sim \frac{\rho_j (v_j - v_h)^3 A_j}{(v_j - v_h)} = \Pi_{ram} \sim \rho_{ext} v_h^2 A_j, \tag{19}$$

where L_j is the jet's kinetic luminosity, v_j the flow velocity, v_h the head's advancing velocity, and ρ_j and ρ_{ext} the jet's and ambient matter's density, respectively. Then, with $\nu = \rho_{ext}/\rho_j$, we obtain the typical velocity at which the hot spots plough their way into the external medium:

$$v_h \sim \frac{v_j}{1 + \sqrt{\nu}}, \tag{20}$$

i.e. light jets ($\nu > 1$) are decelerated more than heavy jets ($\nu < 1$). The distance travelled by the hot spot depends on the source's lifetime; it can be much larger than any stopping distance of a single plasmon.

5.2 *Extended Lobes*

The advancing working surface inflates a "cocoon" in the intergalactic medium (IGM) surrounded by a bow shock enveloping the jet channel. The pressure distribution between hot spots and the leading bow shock drives a flow pattern sideways and backward along the jet. The bow shock permits the internal jet pressure and external IGM pressure to balance through appropriate gradients in their macroscopic quantities. In fact, the cocoon wraps the entire radio source (Begelman & Cioffi 1989). Therefore, the cocoon's width is determined by the

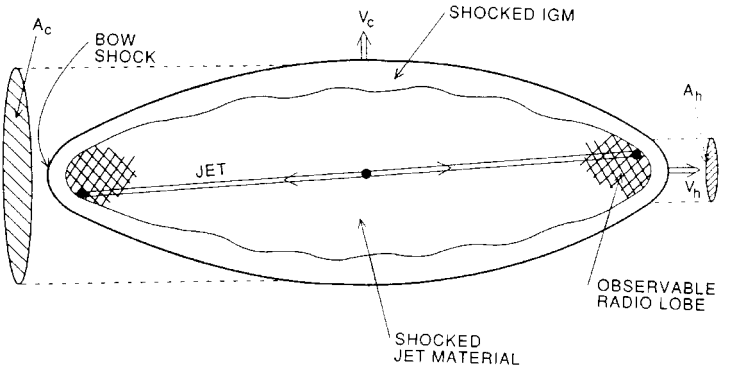

Figure 7 Schematic diagram of overpressured cocoons around jets (Begelman & Cioffi 1989).

drive of its internal pressure expanding in the external medium at sonic speeds (its length is given by the hot spots' advancement).

This situation has been modeled by Begelman & Cioffi (1989) and Cioffi & Blondin (1992); Figure 7 is a cartoon drawn from these references. The head of the bow shock can have a cross section $A_h \geq A_j$ if the jet direction fluctuates on short time scale; in this case, the advancement velocity v_h, as determined by the modified balance Equation 20, becomes the following for light jets ($v_j \gg v_h$):

$$v_h \sim \left(\frac{L_j}{\rho_e v_j^3 A_h}\right)^{1/2} v_j \sim \left(\frac{\rho_j A_j}{\rho_e A_h}\right)^{1/2} v_j. \tag{21}$$

The cocoon pressure P_c drives a sideways shock into the IGM at a speed v_c that is fixed by the balance of P_c and ram pressure $\rho_e v_c^2$; in the approximation that the cocoon inflates at constant L_j and v_h, $P_c \sim L_j T / A_c v_h$, where A_c is the cocoon's cross section. Then,

$$v_c \sim \left(\frac{L_j v_j A_h}{\rho_e}\right)^{1/4} t^{-1/2}, \tag{22}$$

until it decreases below the speed of sound c_s in the IGM. The cocoon is elongated, $v_h \geq v_c$, when $L_j \geq \rho_e v_j^3 A_h^3 / A_c^2$, where A_c is the cocoon cross section. The whole body of the radio galaxy becomes embedded in an overpressured region, and this makes the jet collimation easier: Observationally, we cannot measure the gas pressure in the cocoons owing to the limited angular resolution of X-ray telescopes, but jet confinement may actually come from the regions of the cocoon at the interface of the flow. In addition, the transverse dimensions of lobes are due to the bow shock expansion and are made wide through wave propagation.

5.3 *Filaments*

We mention above that a synchrotron "thermal" instability excites compressional modes with a wave vector transverse to the local magnetic field, leading to filamentary structures parallel to the field. These structures are nonstationary and evolve rapidly at the time scale of synchrotron emission. Numerical results by Bodo et al (1992) have shown that the nonlinear development of the instability makes the filaments brighter than the background if a continuous supply of (reaccelerated) relativistic electrons is guaranteed. In terms of time scales of particle diffusion, the origin of these fresh particles could be the hot spots themselves, when present, or weak shocks in a turbulent medium.

5.4 *Numerical Models of Jet's Head Evolution*

The nonlinearity and interaction of the physical processes invoked requires a numerical approach. The pioneering work in the field was done by Norman et al (1982), who simulated (from a PPM code) the basic features and components described above.

TWO-DIMENSIONAL SIMULATIONS Two types of geometrical configurations have been studied in some detail: cylindrical jets and slabs. In the first case, only axisymmetric features can be studied (i.e. pinches), while slabs give a preliminary view of the development of wiggles in the flow. The main results obtained are listed in the following subsections.

Working surface and cocoon The jet deceleration is accomplished by a strong perpendicular shock at the front interface with the external medium (Mach disk), which thermalizes its bulk kinetic energy. The advancing working surface creates a bow shock in the ambient plasma, exactly as in the radio sources. Light jets ($\rho_{ext}/\rho_j > 1$) display an extended overpressured region inflating behind the bow shock, usually called the cocoon, while heavy jets ($\rho_{ext}/\rho_j < 1$) appear not to have a cocoon (Norman et al 1983). The cocoon is formed initially by shocked jet material compressed at the Mach disk that feeds a backflow along the sides of the jet. Then the bow shock expands in the external medium and is ram-pressure confined; expansion stops when its pressure has decreased to match the external pressure. In the case of highly supersonic light jets, Loken et al (1992) showed that the overpressure factors can be as high as a few thousand, yielding collimation of the jet over its entire length. On the other hand, the extension of the cocoon overall is smaller than in the case of slightly supersonic jets.

Internal shocks The backflow generated at the working surface is characterized by quasiperiodically formed vortices that pinch off the jet behind the Mach disk and excite Kelvin-Helmholtz reflected modes at the contact surface; hence, internal oblique shocks develop in the recurrent pattern already found for infinite collimated flows (Norman et al 1983).

Intermittent jets Clarke & Burns (1991) have analyzed the effects of intermittency of injection. Reborn jets are relatively short-lived as they must propagate in the wake of previous outflows encountering a hot light plasma; consequently, they are dense jets and advance quasiballistically.

Jitters Burns et al (1991), using a slab geometry, have experimented with the effects of jitters on the injection direction and found that lobes may be more extended than predicted by diffusion of the overpressured cocoon. In fact, nonaxisymmetric kink body modes can amplify the initial jitter and produce large vortices in the lobes. Associated hydrodynamic mechanisms can then develop a complicated web of filaments and weak shocks similar to what is observed in radio sources.

External medium Most simulations are performed for jets in pressure equilibrium with the external medium or for overpressured jets in a homogeneous external medium. The effects of inhomogeneities in the ambient medium along the jet path have been addressed by Norman et al (1988) and Gouveia Dal Pino et al (1996). For instance, they showed that, when a jet crosses a shock wave in the external medium because of a preexisting supersonic wind, an internal Mach disk can form that causes a sudden transition to a subsonic, turbulent trail with extended mixing and entrainment. The condition for disruption is $M_j/M_{wind} < 1$ upstream of the shock. The results of simulations are very similar to the morphology of wide-angle–tail (WAT) sources. Decollimation of light jets ($\rho_j < \rho_{ext}$) is also produced by steep negative pressure gradients in the external medium: Broad relaxed cocoons are formed where the Mach disk is very weak, and no internal shocks are transmitted to the jet. On the opposite side, positive pressure gradients compress and collimate jets and produce wiggling and pinching instabilities.

Relativistic jets Relativistic jets have been simulated by Martí et al (1994) and by Duncan & Hughes (1994) for low Mach number jets and by Martí et al (1995) for high Mach number jets. The same global phenomenology of classical nonrelativistic jets is displayed in their results. However, in contrast to classical simulations for high-velocity jets, these authors determined that relativistic jets propagate more efficiently into the external medium following approximately the analytic result

$$v_h = \frac{v_j}{1 + \sqrt{v}[1 - (v_j/c)^2]^{1/2}}, \tag{23}$$

which yields higher advancement velocities as compared with Equation 20. The Mach disk inflates large overpressured (up to 30 times) cocoons and excites a rich pattern of internal oblique shocks. However, a word of caution must be added to these results, as the authors' grid resolution is rather poor and may not reproduce accurately the boundary layer between the jet and ambient medium.

Radiative jets The assumption of adiabatic jets is obviously untenable from the astrophysical point of view. In addition, mapping of the radiation field is necessary to make a comparison with observations. Several simulations include thermal radiative cooling by atomic transitions. Radiative cooling develops dense cool shells at the working surface and induces typically smaller cocoons. This result produces loose collimation and decreases the number and strength of internal shocks (Blondin et al 1990). On the other hand, extragalactic radio sources emit nonthermal synchrotron radiation principally. This is somewhat more difficult to calculate, as it requires understanding the formation of the suprathermal relativistic tail of the electron distribution function, which is most likely supported by acceleration processes of shocks and turbulence (see next section). Here, we remark that, following the results already obtained for infinite jets, the effect of radiative losses towards the dynamical evolution of extended radio sources does slightly affect the overall phenomenology and simply slows down the evolution of instabilities and turbulent mixing. However, a better understanding of the interaction between the thermal and nonthermal plasma components is required before these conclusions can be accepted. In addition, as magnetic fields are necessary for synchrotron emission, MHD models are specifically required.

A detailed solution In a recent analysis based on a high-resolution 2-D hydrocode of the PPM type, Massaglia et al (1996a) have calculated in much detail the dynamics of the interaction with an extensive exploration of the parameter space especially toward high Mach numbers and for light jets, following the system evolution for long time scales through a specific renormalization algorithm that allows all parts of the cocoon to be kept inside the computational domain. The integration was performed over the full set of adiabatic, inviscid fluid (Euler) equations. In order to follow the mixing and entrainment effects between jet and IGM, an additional advection equation is solved for a scalar field, f, initially set equal to 1 inside the jet and ϕ outside. A collimated flow is injected from one side of the domain boundary into a medium at rest and in pressure equilibrium. The velocity and density profiles transverse to the jet are constant, rapidly changing to external values across the interface. Free outflow boundary conditions are used everywhere apart from the orifice where the jet enters.

Five different regions appear: (*a*) the jet; (*b*) the shocked jet material still flowing in the forward direction; (*c*) the shocked jet material reflected backwards at the contact discontinuity and flowing back at the jet side; (*d*) the shocked external material; (*e*) the unshocked external material. The shocked backflow and external material form the cocoon. The high-pressure cocoon squeezes the jet and drives shock waves into it, which reflect on the axis and assume the characteristic biconical shape. The aspect of the interaction depends on M_j: A stronger interaction between biconical shocks and jet head is

obtained for high M_j (Figure 8). The dependence on ν is much weaker (for light jets). The jet thrust is modulated by the biconical shocks impinging on its head, and this can produce a periodic increase in the advance velocity of the head, leading to a strong change in the cocoon morphology.

The jet's head advances, generally following Begelman & Cioffi's (1989) solution over the following time scales:

$$\tau = t\frac{M_j}{1+\sqrt{\nu}}, \tag{24}$$

but several significant differences appear. Two classes of dynamical evolution are found: (*a*) Jets with high M_j and ν have faster v_h and show recurrent acceleration phases such as those due to strong thrust by the biconical shocks; (*b*) jets with low M_j and ν have slower v_h, as the shock thrust is weak. The critical parameter is the inclination angle of the biconical shocks that determine the thrust behind the head. Oblique shocks must have a small inclination angle on the axis in order to produce a strong acceleration effect.

The cocoon's evolution follows the head's, but the influence of the density contrast is stronger. Again, two classes are found (Figure 9): (*a*) fat cocoons, which are more extended laterally; (*b*) spear-headed cocoons, bearing the sign of the recurrent acceleration of jets with high M_j. The system dynamics can be understood by following the behavior of the tracer f, which provides snapshots of the spatial distribution of the jet particles. Slow jets and fast jets with high density ratios behave differently from fast jets with low density ratios (Figure 9).

For high Mach numbers, $M_j = 100$, the shock that surrounds the cocoon engulfs matter of the external ambient medium. If this shocked region becomes the site of particle acceleration, we can say that the form of the lobe resembles the density distribution of Figure 9*a*, with an elongated structure that has the front part protruding from the lobe. Similar morphologies can be found in the sample of high luminosity radio sources by Leahy & Perley (1991); representative examples are 3C42, 3C184.1, 3C223, 3C441, 3C349, and 3C390.3. In the case of slower jets, shocks form only in the frontal part of the cocoon; therefore, the actual lobe has to have a morphology similar to that given by the tracer in Figure 9*a*,*b*. Examples of this second type of morphology can be found in the same sample: 3C296, 3C296, and 3C173.1 are good examples of this class; the remaining sources of the sample are more irregular.

THREE-DIMENSIONAL SIMULATIONS The morphology of radio lobes is obviously dominated by 3-D effects, which, however, require powerful massive parallel supercomputers for their simulations. For this reason, a full exploration of parameter space in three dimensions has not been completed yet. Historically, the first 3-D simulation applied to astrophysical jets was conducted by Arnold & Arnett (1986) at very low spatial resolution. At present, the most complete

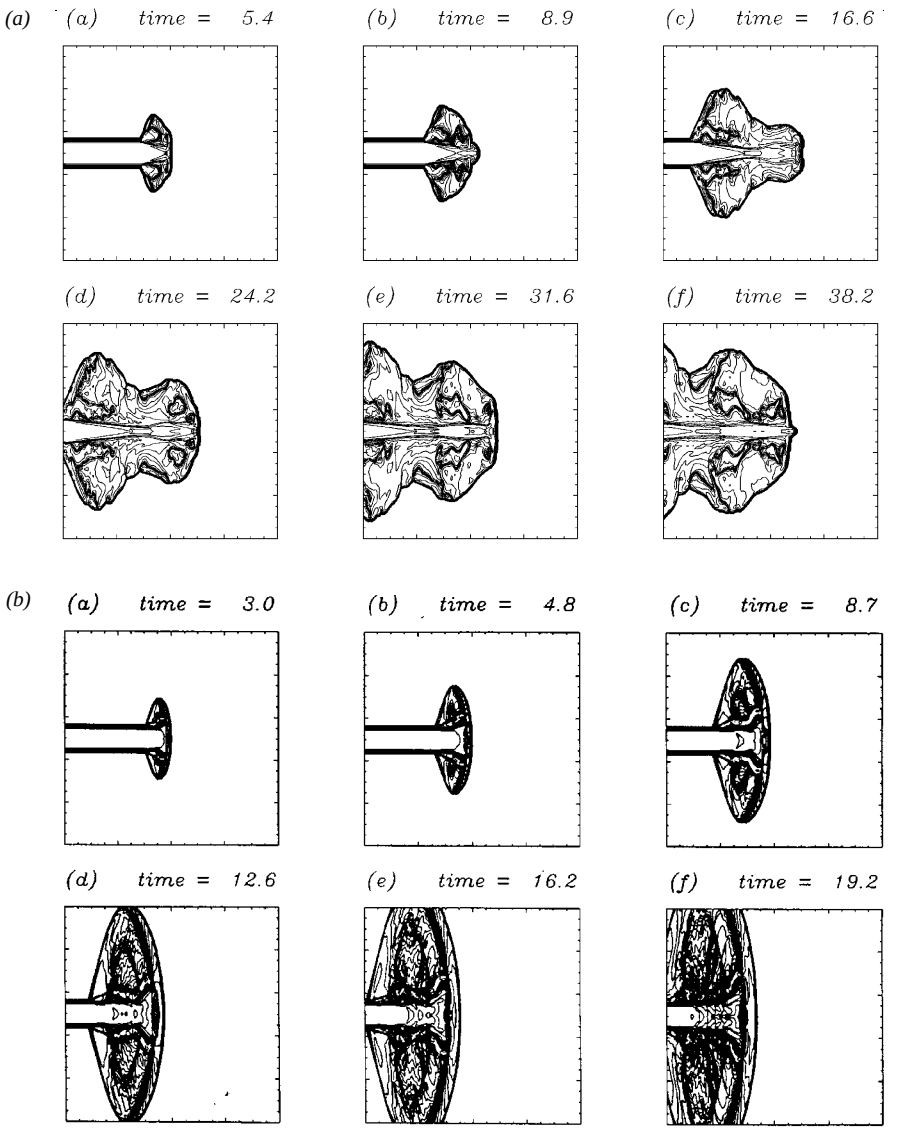

Figure 8 Evolution of jet's head: (*a*) high Mach number jet, (*b*) low Mach number jet (Massaglia et al 1996a). The quantity plotted is the longitudinal momentum flux ρv_z^2.

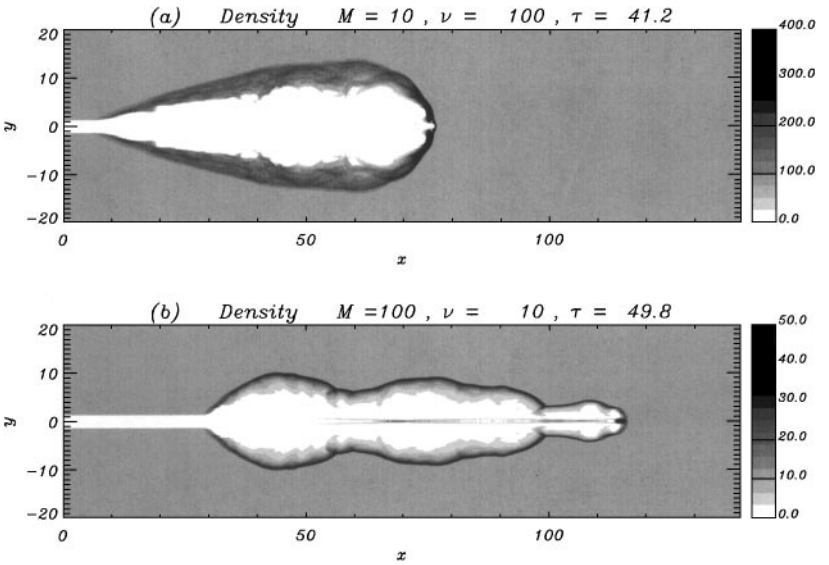

Figure 9 Cocoon morphology: (*a*) high Mach number, high density contrast, (*b*) high Mach numbers, low density contrast (Massaglia et al 1996a).

simulations in fully 3-D geometry are by Clarke (1996) and Norman (1996), both using PPM-type codes (ZEUS-3D and CMHOG).

Light ($\rho_j \sim 10^{-2}\rho_{ext}$) and moderately supersonic ($M_j \leq 10$) jets have been considered. The resolution adopted is still relatively poor for investigating in detail the physics of boundary layers, mass entrainment, and cocoon turbulence development. In the initial part of the jet, close to the source, the results apparently are not different from the 2-D case. An overpressured cocoon confines the collimated flow. However, a strong turbulent mixing between jet and ambient material occurs, characterized by small scale-vortices, whereas in 2-D simulations, large-scale ones were dominant; this is a well-known difference in the 2-D and 3-D turbulence cascades. The important result is that mixing does not reach the very backbone of the jet, and the cocoon ends up being overdense. The jet is more efficiently protected from disruption than 2-D results predict (or in predictions of the Kelvin-Helmholtz instability analysis of the previous section), although the usual sequence of oblique internal shocks appears.

The jet starts displaying large perturbations a few cocoon radii behind the leading working surface. Instead of the Mach disk, now a less well-defined termination shock accomplishes the transition to subsonic flow and bow shock. In addition, the jet displays a vigorous "flapping" of its head and is deflected 4–5

times before it advances by about a cocoon radius. This flapping is a 3-D process that is due to the cocoon turbulence, which causes irregular deflections of the leading part of the flow and in fact drives the "dentist drill effect" phenomenologically discussed by Scheuer (1974) as a way to increase the extremely small transverse dimensions of radio lobes in highly supersonic jets. Correspondingly, the lack of concentration in the jet head thrust slows down the working surface advancement speed to about half of the ram pressure estimates. Some recurrent reacceleration events of the type described in 2-D results occur also in 3-D scenarios. Norman & Balsara (1993) have simulated the propagation of a jet through a shocked external wind in three dimensions also. Bending and flaring of the jet are found again, showing that the interaction with the external medium can appreciably change the appearance of the physical phenomena.

EFFECTS OF MAGNETIC FIELDS Toroidal magnetic fields, consistently generated in the jet by a longitudinal axial current, confine the plasma through a radial $\mathbf{J_0} \times \mathbf{B}$ force and, in the pure MHD limit, do not allow the formation of large cocoons, as the backflow and return current are small and constrained to the very surface of the jet (Clarke et al 1986, Lind et al 1989). The shocked material at the working surface accumulates in a protruding nose cone because the radial current at the Mach disk gives rise to a forward longitudinal $\mathbf{J_r} \times \mathbf{B}$ force. Therefore, magnetically confined jets would appear lobeless with bright noses and internal knots; this is in contrast with most radio source observations. However, laboratory experiments indicate that plasma columns are unstable to pinch and hose instabilities on dynamical scales, and this should make magnetic noses transient structures. Clarke (1994) has extended the simulation to three dimensions and has confirmed that the nose is disrupted before becoming too long; its final appearance resembles an asymmetric compact lobe with a well-ordered magnetic field and strong polarization, as in quasar jets.

Longitudinal (poloidal) magnetic fields also have been used in simulations to enhance the emission component on the jet axis where the toroidal component vanishes. Kössl et al (1990) have shown that equipartition or weaker helical fields make the flow resemble purely hydrodynamic simulations, apart from a smaller cocoon and slower head advancement. The magnetic field ends up much less ordered and confined on the edges, as in classical FR I radio galaxies.

Koide et al (1996) have addressed the simulation of relativistic MHD flows in slab geometry that are injected parallel to a preexisting homogeneous magnetic field. They used a Lax-Wendroff code with rather low spatial resolution. In the case of a weak magnetic field, a backflow forms along the jet and spreads into a cocoon, which is very similar to what is found in the pure hydrodynamic case. In the case of a strong magnetic field, no backflow and cocoon are formed at all. In both cases, however, the magnetic field is reversed at the beam surface. The overall result is that relativistic magnetized jets are well collimated

and propagate without slowing down. In a subsequent paper, Nishikawa et al (1997) extended the study to 3-D relativistic MHD with a bulk Lorentz factor of 4.56 and in pressure equilibrium with the external medium. Three-dimensional (3-D) relativistic beams decelerate more efficiently than 2-D ones, are better confined, develop weak internal structures, and are associated with smaller bow shocks, thinner cocoons, and weak backflows. Koide et al (1996) have also considered jets propagating at an angle with respect to the external magnetic field and found that all jets for any Mach number are bent and, in some cases, also split. The working surface contains a compressed magnetic field and the head advancement speed is reduced. These results might explain some aspects of the phenomenology of BL Lacs.

A fully relativistic MHD code has been developed by van Putten (1996) and works at higher resolution and precision, especially at shock discontinuities. It has been applied to the standard 2-D light jets, assuming a toroidal confining magnetic field out of radial force balance at the injection point. This drives the formation of a nozzle and knots along the jet until a termination Mach disk accomplishes the deceleration. Downstream of the Mach disk, the flow bifurcates into a forward nose cone and a backflow, exactly as in the nonrelativistic case. The cocoon remains relatively small, but again, these simulations span short time scales only; perhaps they are relevant to interpreting the class of compact steep spectrum (CSS and CSO) objects.

5.5 *Understanding Jet Microphysics*

The above numerical experiments qualify the classical continuous jet model to explain the basic observational characteristics of extended radio sources. On the other hand, our quantitative understanding of the interlacing physical processes is still preliminary. For instance, the activity of the working surface and the formation and expansion of the cocoon are typical examples of boundary layer physics with instabilities, mixing, turbulence, etc. So far, these conditions have been simulated in a hydrodynamic or MHD approximation, while most of the important processes are plasma effects. On the other hand, plasma simulations are at present prohibitive over time scales of a few proton gyroradii for any available supercomputer. A possible approach that should be tested soon is a two-fluid model in which currents are included explicitly and the interaction between electrons and ions is taken into account for an explicit calculation of the transport coefficients, diffusion, resistivity, thermal conduction, etc.

Along the same lines, hydrodynamic or MHD models cannot properly represent crucial physical elements as currents and electromagnetic fields. The only attempt to deal with this problem is by Clarke et al (1986). However, those authors assumed an unmagnetized external medium so that the jet magnetic field cannot diffuse outside its boundaries and, although it insures collimation, does not participate in the formation of the boundary layer.

Benford (1978) pointed out that current-carrying jets may be naturally self-confined by azimuthal magnetic fields closing inside an extended cocoon that is transporting a return current. In such a scheme, Jafelice & Opher (1992) examined the radial evolution of the plasma discharge generated in the ambient plasma by a charged jet, assuming that the return current is diffused over an extended region defined by a balance between the gravitational pull and the effect of the Lorentz forces.

When a current-carrying jet is injected into a plasma, electron currents are induced to flow in such a way that they oppose the self-magnetic field (Miller 1982). Depending on the plasma conductivity σ, the induction electric field of the jet can effectively cause the net (jet plus plasma) current to vanish. For small resistivity, the induced current remains concentrated within the boundary layer of the jet; otherwise, it can diffuse over a large region around the jet. This leads to substantial differences in the physics of charged jets with respect to neutral jets. For instance, if the jet current in cylindrical geometry is assumed to have a form

$$J_{jz} = \frac{I_j}{\pi R^2(t)} e^{-r^2/R^2} \Theta(t - z/v_j), \tag{25}$$

with $\Theta(y)$ as the step function; then the response plasma current is calculated to be

$$\begin{aligned} J_{pz} &= J_1 + J_2 \\ &= -J\,(t_*) - \int_0^t dt' \left(\frac{2\dot{R}}{R}\right)\left(\frac{r}{R}\right)^2 \frac{J^*(t-t')}{1+(t-t')/\tau_d} \Theta(t' - z/v_j), \end{aligned} \tag{26}$$

where

$$J(t_*) = J[R\,(t_*), t - t_*] = \frac{I_j}{\pi R^2(t_*)} \frac{e^{-[r^2/R^2(t_*)(1+(t-t_*)/\tau_d)]}}{1+(t-t_*)/\tau_d}, \tag{27}$$

with $t_* = z/v_j$ and $\tau_d = 4\pi\sigma R^2/\mathrm{c}^2$. The consistent magnetic field is

$$B_\theta(r) = -\frac{\partial A}{\partial r} = \frac{1}{r}\int_0^r dr\, r(J_{jz} + J_1 + J_2). \tag{28}$$

If the jet contracts under the self-pinching action of the azimuthal magnetic field consistent with the carried current, then $dR/dt < 0$ and $J_2 < 0$, and the return current is less, which focuses the jet more. The reverse case, which might be expected from a jet that is small at the head and grows larger behind it, $J_2 > 0$ and the return current is preferentially driven in the region outside the radius $R(t)$. This case may correspond to a return current sheath around

the jet. The radial distribution of J_2 is peaked at the edge of the jet because it is driven by the expansion/contraction of the radius.

Further behind the working surface, the plasma current is dissipated by ohmic losses. Following Lovelace & Sudan (1971), the energetics can be evaluated in terms of the Poynting theorem. If a sharp front of considerable energy γ_0 (in units of mc^2) is considered, the jet velocity changes little in the setting up of the jet current system:

$$\frac{\delta v_j}{v_j} \approx \frac{\delta \gamma}{\gamma^3} \ll 1, \tag{29}$$

and the beam current itself is almost constant $\partial \mathbf{J}_\mathrm{j}/\partial \mathbf{t} \approx 0$ and $\partial \mathbf{B}_\mathrm{j}/\partial \mathbf{t} \approx 0$. The jet loses energy as

$$\frac{d\epsilon_j}{dt} = -\int dA\ \mathbf{J}_\mathrm{j}(\mathbf{t}) \cdot \mathbf{E}, \tag{30}$$

where $\mathbf{E}$ is the induction electric field and the integral is over the jet cross section A. Therefore, the plasma magnetic field decays behind the front and does not exactly counter the jet field because of resistive decay or other dissipative effects, so that

$$\mathbf{B}_\mathrm{p} = -g\mathbf{B}_\mathrm{j}, \quad \mathbf{J}_\mathrm{p} = -g\mathbf{J}_\mathrm{j}, \quad \mathbf{B} = (1-g)\mathbf{B}_\mathrm{j}, \quad \mathbf{J} = (1-g)\mathbf{J}_\mathrm{j}, \tag{31}$$

with $g \leq 1$. Then, writing the energy stored in the full self-magnetic field as

$$U_j = \int dA\ \frac{B_j^2}{8\pi}, \tag{32}$$

we can express the quick equilibrium setup (corresponding to the current or magnetic field decay) using the Poynting theorem. We then obtain the total energy dissipated by the interaction of the current with the induced field $\mathbf{E}$:

$$-\int dA \mathbf{J_j} \cdot \mathbf{E} = \int dA \frac{\mathbf{B}_\mathrm{j}}{4\pi} \cdot \frac{\partial \mathbf{B}}{\partial \mathbf{t}}. \tag{33}$$

Integrating over the setup time Δt with $\mathbf{B_j}$ constant gives

$$\begin{aligned}
\epsilon_{diss} &= \left[\int dA \frac{B_j^2}{4\pi} + \int dA \frac{\mathbf{B_j} \cdot \mathbf{B_p}}{4\pi} \right]_t^{t+\Delta t} \\
&= \left[2U_j + \int dA \frac{\mathbf{B_j} \cdot (-g\mathbf{B_j})}{4\pi} \right]_{[t+\Delta t]} - \left[2U_j + \int dA \frac{\mathbf{B_j} \cdot (-\mathbf{B_j})}{4\pi} \right]_t \\
&= 2(1-g)U_j.
\end{aligned} \tag{34}$$

A fraction $(1+g)/2$ of the total dissipated energy goes into the plasma through inductive ohmic heating, independent of the conductivity, as the return current decays; this occurs as g evolves from 1 to nearly zero as time approaches the magnetic diffusion time for the relevant distance scale. Also, a fraction $(1-g)/2$ goes into the creation of magnetic fields. All this occurs over the relevant distance for magnetic diffusion, and so such estimates are qualitatively correct if decay occurs in small filaments built up by filamentary instability very near the jet head. Energy deposition in the plasma appears as raw heating and as electrostatic fields driven by plasma instabilities, which eventually will decay into further heating. This is the final state of the electrodynamic braking of the jet. Such qualitative considerations apply to "sudden" jets, which induce return currents across their cross sections, setting up the return current path within or very near the jet area. This is because the "skin effect" of rapid induction confines currents to within a short distance of the jet radius. Such a picture applies best to very fast (perhaps relativistic) jet heads, which then are slowed quickly by inductive braking and suffer filamentary instability as well.

A different situation envisions a jet that builds gradually, so that inductive energy does not have to drive return currents within the narrow channel of the jet radius but rather does so over the expanded jet head. This requires much less energy investment, since the return current is carried by a far larger number of electrons across a broad cocoon that has a typical radius comparable to the jet head. The energy invested in setting up the return current system over a large cocoon radius is given by the ratio of the total charge carriers (electrons) carrying the jet current (N_j) compared to the number within the cocoon radius carrying the return current (N_p):

$$\frac{\epsilon_p}{\epsilon_j} = \frac{N_j}{N_p g^2} \ll 1. \tag{35}$$

Since $g = 1$ at the beginning of the return current setup, large cocoon radii are energetically preferred, and as g falls, more energy must be invested by the entire jet system to maintain itself against diffusion of return current outward while maintaining self-confinement at the jet core. Such scenarios suggest that jets may begin as narrow, fast (perhaps relativistic) flows, but inductive braking slows them until their heads are broad enough to develop larger inductive return current systems. Then they acquire cocoons of backflowing plasma. This links the inner jet, which is self-confined by the greater self-field near the center, to the outer cocoon, where the eventual return currents primarily flow. Such cocoons have substantial stabilizing powers, as they inhibit lateral instability by adding the cocoon mass to the jet, increasing its inertia.

6. RADIATION AND PARTICLE ACCELERATION IN LARGE-SCALE JETS

The spectral and polarization characteristics of jets, from radio to X and γ rays, are consistent with emission by a power-law distribution of relativistic electrons over the whole frequency range, i.e. γ_{el} up to 10^7 in some cases. Meisenheimer et al (1996) have combined detailed data on the M87 jet over the whole frequency range from radio to X rays. They showed that the spectral profile is very uniform along the jet, corresponding to a power-law electron distribution $N(\gamma) \propto \gamma^{-2.3}$ for the synchrotron model in a uniform magnetic field. Similarly, the high-frequency cutoff in the synchrotron spectrum is very nearly constant, and this uniformity applies down to the smallest scale, $l \sim 10$ pc, that can be resolved. Such frequency corresponds, at equipartition, to an electron upper Lorentz factor $\gamma_c = 9 \times 10^5$. They concluded that reacceleration must be independent from local parameters, as high brightness knots have the same spectrum of low brightness knots. The favored acceleration mechanism should then be of "universal" type. Acceleration by MHD turbulence and shocks are the best candidates to produce a "universal" particle energy spectrum (Bodo et al 1995, Meisenheimer et al 1996b, Ferrari & Melrose 1997).

In the original twin-jet model, radiation was attributed to relativistic electrons reaccelerated in shocks at the hot spots and working surface. Blandford & Ostriker (1978) showed that shocks under rather general conditions produce power-law spectra with slope $\sim$2–3, depending on the shock strength, in agreement with the observed radiation spectral index $\sim$0.5–1. In connection with acceleration by turbulent MHD modes, Ferrari et al (1979), Eilek (1979), and Lacombe (1977) have calculated the time scales of nonlinear coupling of modes, showing how these modes can guarantee a constant input of energy toward particle acceleration. Benford et al (1980) proposed a scenario in which long wavelength unstable MHD modes start a nonlinear cascade toward short wavelength modes and support a Fermi-like acceleration of electrons. Instead of considering instabilities as events that can destroy jets, they must be examined in their positive aspect. Perturbations can grow to shocks and at the same time can cascade energy down to the level of turbulent modes and also eventually couple to radiative modes.

The main question in accelerating electrons is the need for an injection mechanism of already relativistic electrons. In fact, the condition for resonant interaction of electrons with Alfvèn or fast magnetosonic waves (necessary both for stochastic acceleration by turbulent modes or for scattering/trapping across shock discontinuities) is approximately $\gamma_{\min,e} \sim (v_u/c)\,(m_p/m_e) \gtrsim 1$, where v_u is the upstream flow speed (Eilek & Hughes 1991). Injection mechanisms proposed are runaway DC electric fields, electrodynamic forces in current-carrying flows, magnetic field reconnection, shock drifts, etc. The subject has

not been explored self-consistently so far. Stochastic acceleration of thermal protons/ions is instead possible; therefore, a situation should be analyzed in which ions are accelerated to ultra-relativistic energies and drag with them electrons via electrostatic instabilities.

A quasi–loss-free transport of particles from the AGN cores to the extended lobes is a possible alternative to reacceleration. Felten (1968) devised two basic scenarios: 1. Jets contain a component of ultrarelativistic protons/ions responsible for carrying the main fraction of energy and momentum that can then be converted into secondary electrons along the jet (Mastichiadis & Kirk 1995); 2. jets contain ultrarelativistic electron/positron pairs carrying the bulk flow and inertia and at the same time providing synchrotron emission (Kundt & Gopal-Krishna 1980).

6.1 *Evolution of the Relativistic Electron Distribution Function*

Self-consistent particle acceleration and radiation loss processes have not been fully implemented in numerical dynamical codes, although radiation losses have been proven to influence the dynamics by slowing down the evolution of perturbations (Rossi et al 1997). Radiation has been generally estimated by just assuming that synchrotron emissivity is proportional to the local pressure, which is consistent with pressure equipartition between thermal and nonthermal components (Komissarov & Falle 1997).

Massaglia et al (1996b) have developed a self-consistent method to calculate numerically the time evolution of the relativistic electron component in a supersonic jet exposed to adiabatic losses, synchrotron emission, and acceleration at shock discontinuities. The numerical method solves the Kardashev equation for the relativistic electron distribution function $F(E)$ that is assumed to move along with the thermal component dominating the dynamics:

$$\frac{DF}{Dt} = \frac{\partial}{\partial E}[(-\alpha E + \beta E^2)F], \tag{36}$$

of which the first term on the right corresponds to adiabatic losses, $\alpha = -(\nabla \cdot \mathbf{v})/3$, and the second to synchrotron losses, $\beta = bB^2$; D/Dt is the Lagrangian derivative. This equation can be solved to

$$F(E,t) = KE^{-\gamma}[1 - a_1 e^{-a_2} E]^{\gamma-2} e^{(\gamma-1)a_2}, \tag{37}$$

subject to the condition $F(E,0) = K_0 E^{-\gamma}$ and with the integrals along the fluid element trajectory:

$$a_1 = \int_0^t \beta e^{-a_2} dt \quad a_2 = \int_0^t \alpha dt. \tag{38}$$

Therefore, the spectral distribution can be followed solving for a_1 and a_2 together with the system of the fluid equations in the assumption that relativistic

electrons are tied up with the thermal plasma. In addition, the authors considered a systematic shock acceleration that prescribes that where the flow develops a shock discontinuity, the particle energy is increased by a given factor proportional to the shock compression. The dynamical code employed was a standard hydrodynamic PPM with a passive magnetic field whose evolution follows a scalar advection equation. Magnetic field, synchrotron emissivity, and cutoff frequency are plotted in Figure 10 for two cases of supersonic light cocoons. Calculated spectral profiles suggest that injection of high-energy particles is the critical element to reproducing observational data.

Ferrari & Melrose (1997) calculated the particle spectrum produced by MHD turbulence from the lower cutoff fixed by the injection mechanism and the upper cutoff related to radiation losses:

$$\gamma_{\max} = \left[\frac{9\pi}{8}\frac{u_s^2}{r_e c\Omega_e}\left(\frac{\delta B}{B}\right)^2\right]^{3/4}(k_0 r_0)^{1/2}\,. \tag{39}$$

With standard observational parameters for M87, $u_s \sim 10^{-2}c$, $B \sim 30$ nT, $r_0 \sim 6\times 10^6$ cm, and for a well-developed Kolmogorov turbulence, $(\delta B/B)\sim 1$, with energy input on the largest correlation scale $L_0 = k_0^{-1}$ cascading to smaller scales. Then $k_0 r_0 \sim 2\times 10^{-12}/L_{0,pc}$, where we have measured L_0 in parsecs, and Equation 39 gives $\gamma_{\max}\sim 10^6/L_{0,pc}^{1/2}$, which for $L_{0,pc}\sim 1$ is close to the required value quoted by Meisenheimer et al (1996). This indicates that turbulence must have a correlation length of at most 1 pc. This is a prediction to be tested by future high-resolution observations.

6.2 *Comments: Beaming Effects in Relativistic Outflows*

VLBI observations of proper motions in the cores of radio galaxies and quasars have shown that compact radio jets possess bulk Lorentz factors up to $\gamma_{bulk}\sim 10$ (Zensus 1996). However, intraday variability (IDV) of some compact radio sources may also be claimed as indirect evidence of highly relativistic flows (Qian et al 1991, Quirrenbach et al 1989, 1991, Witzel 1992). Begelman et al (1994) show that, in order to interpret these rapid variabilities in terms of an incoherent synchrotron-emitting jet with non–self-absorbed convected disturbances, the required Lorentz factors are very high, up to 10^3. In addition, the emitting disturbance must be close to the self-absorption limit, and this reduces the emission efficiency. Even relatively "normal" sources would correspond to jet powers $L_j \geq 10^{47}$ erg s^{-1} above the Compton catastrophe limit. Such Lorentz factors would rule out any kind of radiative or thermal jet acceleration, favoring hydromagnetic acceleration (Begelman et al 1994). For highly beamed radiation in the AGN cores in the framework of unification models, we refer to the review by Ulrich et al (1997).

A possible resolution of the serious limitations of the incoherent synchrotron model is to refer to coherent emission from plasma oscillations. Benford (1992)

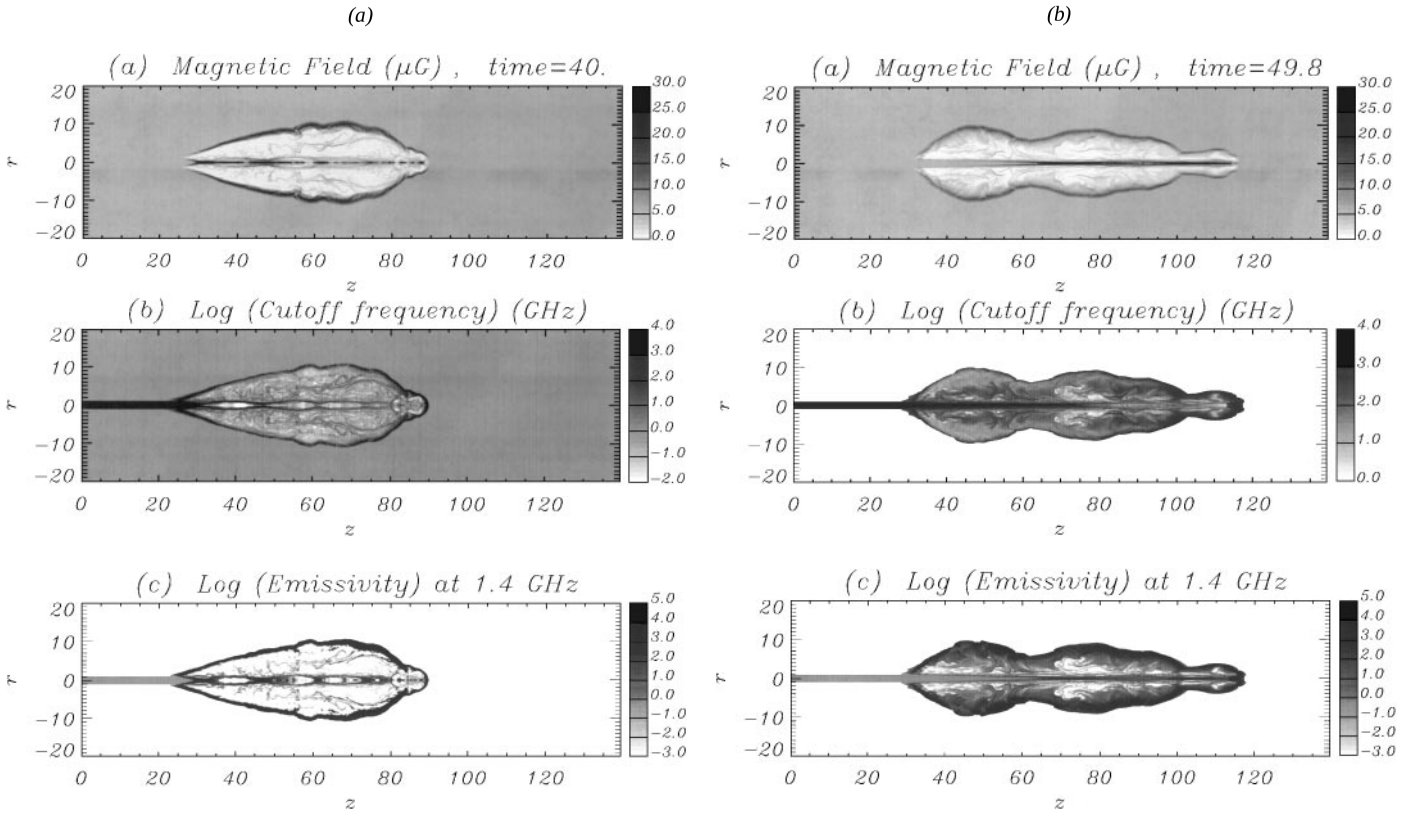

Figure 10 Synchrotron radiation from jets and cocoons: (*a*) $M = 300$, $\nu = 100$; (*b*) $M = 100$, $\nu = 10$ (Massaglia et al 1996b).

has discussed this solution with reference to laboratory experiments that show how very high brightness luminosities can be achieved. Stimulated Compton scattering in the deep cores of AGNs could, however, prevent this radiation from escaping (Coppi et al 1993).

6.3 *Acceleration of Cosmic Rays in Extragalactic Radio Sources*

Jets and cocoons have also been invoked to explain the question of production of ultra–high-energy cosmic rays (UHECRs), $E > 4 \times 10^{19}$ up to 3×10^{20} eV, revealed by extensive air shower detectors (Norman et al 1996). The argument is that large-scale shocks produced inside a jet or by the expansion of the working surface and cocoon into the ambient plasma can accelerate already relativistic protons/ions to the maximum energies. The limiting upper energy cutoff is approximately $E_{\max} \simeq ZeB\beta_s R_s$, which yields (in typical units) for hot spots in jets ($R_s \sim R_j$, $\beta_s \sim \beta_j$)

$$E_{\max} \simeq 10^{20} B_{-4} R_{j,1\mathrm{kpc}} \beta_j \text{ eV} \tag{40}$$

and for overpressured cocoons

$$E_{\max} \simeq 5 \times 10^{19} Z B_{-6} L_{46}^{1/2} D_{10\mathrm{kpc}}^{-1/2} n_{-4}^{-1/2} t_{8\mathrm{year}}^{1/2} \text{ eV}. \tag{41}$$

Therefore, hot spots and cocoons appear to be interesting candidates as UHECR sources. Also, the injection problem for ions is less severe than for electrons.

7. OPEN PROBLEMS

Much progress has been made in modeling extragalactic jets in the last few years owing to (*a*) the quantitative and qualitative enrichment of the statistical sample of detailed multifrequency observations and (*b*) the development of reliable numerical codes to simulate the microphysics of supersonic and relativistic outflows. The basic results definitively acquired at present are as follows:

1. Jet acceleration and collimation take place in the inner regions of AGNs through processes in which magnetic fields anchored in accretion disks are the fundamental elements. The disk-jet connection is also operating in other astrophysical conditions, such as binary active stars and star formation regions.

2. Jet propagation survives dynamical and kinetic instabilities due to the interaction with the ambient medium owing to nonlinear effects that create turbulent boundary layers and overpressured cocoons around them.

3. Jet morphologies can be interpreted in terms of the above instabilities connecting shock formation, suprathermal particle acceleration, and synchrotron emission with bright knots, hot spots, bow shocks, and cocoons. The distinction between FR I and II radio galaxies is related to the energy dissipation inside jets, which is parameterized in terms of the flow Mach number and the density contrast with the ambient medium (or cocoon).

4. Doppler beaming is involved in the strong variability of quasars and blazars and may also explain the one-sidedness of strong jets and the global energetics of γ-ray AGNs. This result is, however, still preliminary.

On the other hand, many questions remain open, and more investigations are needed to settle the physics governing fundamental phenomena:

1. Does the bulk flow contain an ion/electron plasma or an electron/positron pair plasma? Originally, the pair plasma was seen as a factor in reducing global energetic demands. Now the question is how efficiently relativistic bulk flows can be produced.

2. How do accretion disks launch collimated flows? Magnetized coronae heated by reconnection of loops buoyant from the accretion disk are perhaps the best candidates, but other processes have not been fully investigated yet, in particular those involving electromagnetic forces and currents. Nor has much progress been made on the (formidably difficult indeed) study of the electrodynamics of black hole magnetospheres.

3. Is a fluid approximation a reliable way to represent the microphysics of jets? Most likely not: Kinetic effects define the transport coefficients and the development of perturbations and nonlinear structures inside the flow. Therefore, the boundary layer at the interface between jets and ambient medium is certainly governed by these coefficients, and so far we have only preliminary indications about their effects on mixing, entrainment, turbulence, etc. A fully kinetic treatment is at present prohibitive; the next possible step may be a two-fluid model implemented in numerical codes that have been adapted to the problem.

4. How important are currents? Given the high conductivity of astrophysical plasmas, the general trend is to neglect charge separation and current effects on large scales. Low return currents can be dispersed over large cocoons with low current densities without perturbing the ambient medium. However, current densities may be very high inside jets and may again influence the transport coefficients and dissipation processes. The above-mentioned two-fluid approach might answer this question.

5. We have very little information about the spatial and spectral distributions of the suprathermal component of relativistic electrons and ions. From the theoretical side, not much effort has been made so far to couple the suprathermal and thermal components and to couple both of them to the emitted radiation.

If a conclusion can be drawn at this stage of modeling astrophysical jets, it might be said that, while 10 years ago most of what had been observed was interpreted at a phenomenological level, today we have a more quantitative understanding. The general picture is rather firm, but most of the microphysics involved are still unsatisfactorily implemented.

ACKNOWLEDGMENTS

This work was supported by grants of the Italian Ministero dell'Università (MURST) at the Osservatorio Astronomico di Torino and by hospitality at the University of California at Irvine and at the Department of Astronomy & Astrophysics of the University of Chicago. The author wishes to thank many colleagues who have shared their interest in the challenging questions of astrophysical jets, in particular, Gregory Benford, Gianluigi Bodo, Silvano Massaglia, Robert Rosner, Paola Rossi, Edoardo Trussoni, and Kanaris, Tsinganos.

Literature Cited

Antonucci R. 1993. *Annu. Rev. Astron. Astrophys.* 31:473
Appl S, Camenzind M. 1992. *Astron. Astrophys.* 256:354
Appl S, Camenzind M. 1993a. *Astron. Astrophys.* 270:71
Appl S, Camenzind M. 1993b. *Astron. Astrophys.* 274:699
Arnold CN, Arnett WD. 1986. *Ap. J. Lett.* 305: L57
Balbus SA, Hawley JF. 1991. *Ap. J.* 376: 214
Basset GM, Woodward PR. 1995. *Ap. J.* 441: 582
Begelman MC, Blandford RD, Rees MJ. 1984. *Rev. Mod. Phys.* 56:255
Begelman MC, Cioffi DF. 1989. *Ap. J. Lett.* 345:L21
Begelman MC, Rees MJ, Sikora M. 1994. *Ap. J. Lett.* 429:L57
Benford G. 1978. *MNRAS* 183:29
Benford G. 1992. *Ap. J. Lett.* 391:L59
Benford G, Ferrari A, Trussoni E. 1980. *Ap. J.* 241:98
Bicknell GV, Begelman MC. 1996. *Ap. J.* 467: 597
Birkinshaw M. 1991. In *Beams and Jets in Astrophysics*, ed. PA Hughes, p. 279. Cambridge, UK: Cambridge Univ. Press
Biskamp D. 1994. *Phys. Rep.* 237:179
Blackman EG. 1996. *Ap. J. Lett.* 456:L87
Blandford RD. 1976. *MNRAS* 176:465
Blandford RD. 1989. In *Theory of Accretion Disks*, ed. P Meyer, W Duschl, J Frank, E Meyer-Hofmeister, p. 35. Reidel: Kluwer
Blandford RD, Netzer H, Woltjer L, eds. 1990. *Active Galactic Nuclei*, 20th Saas Fee Adv. Course. Berlin: Springer-Verlag
Blandford RD, Ostriker JP. 1978. *Ap. J. Lett.* 221:L29
Blandford RD, Payne DG. 1982. *MNRAS* 199: 883

Blandford RD, Pringle JE. 1976. *MNRAS* 176: 443
Blandford RD, Rees MJ. 1974. *MNRAS* 169:395
Blandford RD, Znajek RL. 1977. *MNRAS* 179: 433
Blondin JM, Fryxell BA, Königl A. 1990. *Ap. J.* 360:370
Bodo G, Ferrari A, Massaglia S, Rossi P, Shibata K, Uchida Y. 1992. *Astron. Astrophys.* 256:689
Bodo G, Ferrari A, Massaglia S, Trussoni E. 1990. *MNRAS* 244:530
Bodo G, Massaglia S, Ferrari A, Trussoni E. 1994. *Astron. Astrophys.* 283:655
Bodo G, Massaglia S, Rossi P, Rosner R, Malagoli A, Ferrari A. 1995. *Astron. Astrophys.* 303:281
Bodo G, Rosner R, Ferrari A, Knobloch E. 1989. *Ap. J.* 341:631
Bodo G, Rosner R, Ferrari A, Knobloch E. 1996. *Ap. J.* 470:797
Bodo G, Rossi P, Massaglia S, Ferrari A, Malagoli A, Rosner R. 1998. *Astron. Astrophys.* 333:1117
Bridle AH, Fomalont EB. 1976. *Astron. Astrophys.* 52:107
Bridle AH, Perley RA. 1984. *Annu. Rev. Astron. Astrophys.* 22:319
Brown GL, Roshko A. 1974. *J. Fluid Mech.* 284:171
Burbidge GR. 1958. *Ap. J.* 129:841
Burns JO, Norman ML, Clarke DA. 1991. *Science* 253:522
Camenzind M. 1986. *Astron. Astrophys.* 156: 137
Camenzind M. 1998. In *Astrophysical Jets–Open Problems, 3rd Torino Wkshp.*, ed. S Massaglia, G Bodo, p. 3, Amsterdam: Gordon & Breach
Capetti A, Macchetto FD, Axon DJ, Sparks WB, Boksenberg A. 1996. *Ap. J.* 448:600
Carilli CL, Perley RA, Bartel N, Soarthia B. 1996. In *Energy Transport in Radio Galaxies and Quasars, Tuscaloosa Workshop*, ed. PE Hardee, AH Bridle, JA Zensus, ASP Conf. Ser. 100, p. 287. San Francisco: Astron. Soc. Pac.
Chan KL, Henriksen RN. 1980. *Ap. J.* 241: 534
Chandrasekhar S. 1961. *Hydrodynamic and Hydromagnetic Stability*. Oxford: Clarendon
Chiueh T, Li Z, Begelman MC. 1991. *Ap. J.* 377:462
Cioffi DF, Blondin JM. 1992. *Ap. J.* 392:458
Clarke DA. 1994. In *Jets in Extragalactic Radio Sources*, ed. HJ Röser, K Meisenheimer, p. 243. Heidelberg: Springer-Verlag
Clarke DA. 1996. In *Energy Transport in Radio Galaxies and Quasars*, ed. PE Hardee, AH Bridle, JA Zensus, ASP Conf. Ser. 100, p. 311. San Francisco: Astron. Soc. Pac.
Clarke DA, Burns JO. 1991. *Ap. J.* 369:308
Clarke DA, Norman ML, Burns JO. 1986. *Ap. J. Lett.* 311:L63
Cohen MH, Cannon W, Purcell GH, Shaffer DB, Broderick JJ, et al. 1971. *Ap. J.* 170:207
Cohn H. 1983. *Ap. J.* 269:500
Contopoulos J. 1995. *Ap. J.* 450:616
Contopoulos J. 1996. *Ap. J.* 460:185
Contopoulos J, Lovelace RVE. 1994. *Ap. J.* 429: 139
Coppi P, Blandford RD, Rees MJ. 1993. *MNRAS* 262:203
De Young DS. 1976. *Annu. Rev. Astron. Astrophys.* 14:447
De Young DS. 1980. *Ap. J.* 241:81
De Young DS. 1993. *Ap. J. Lett.* 405:L13
De Young DS. 1996. In *Energy Transport in Radio Galaxies and Quasars: Tuscaloosa Workshop*, ed. PE Hardee, AH Bridle, JA Zensus, ASP Conf. Ser. 100, p. 261. San Francisco: Astron. Soc. Pac.
Duncan GC, Hughes PA. 1994. *Ap. J. Lett.* 436:L119
Eilek JA. 1979. *Ap. J.* 230:373
Eilek JA, Caroff LJ. 1979. *Ap. J.* 233:463
Eilek JA, Hughes PA. 1991. In *Beams and Jets in Astrophysics*, ed. PA Hughes, p. 428. Cambridge, UK: Cambridge Univ. Press
Falcke H. 1996. In *Jets from Stars and Galactic Nuclei*, ed. W Kundt, p. 19. Heidelberg: Springer-Verlag
Falcke H, Biermann PL. 1995. *Astron. Astrophys.* 293:665
Falcke H, Gopal-Krishna, Biermann PL. 1995. *Astron. Astrophys.* 298:395
Fanaroff BL, Riley JM. 1974. *MNRAS* 167:31P
Felten JE. 1968. *Ap. J.* 151:861
Feretti L, Fanti R, Parma P, Massaglia S, Trussoni E, Brinkmann W. 1995. *Astron. Astrophys.* 298:699
Ferrari A. 1984. In *Unstable Current Systems and Plasma Instabilities in Astrophysics*, IAU Symp. 107, p. 393. Dordrecht: Reidel
Ferrari A, Melrose DB. 1997. *Vistas Astron.* 41:259
Ferrari A, Trussoni E, Zaninetti L. 1978. *MNRAS* 79:190
Ferrari A, Trussoni E, Rosner R, Tsinganos K. 1986. *Ap. J.* 300:577
Ferrari A, Trussoni E, Zaninetti L. 1979. *Astron. Astrophys.* 79:190
Ferrari AE, Rosner, Trussoni R, Tsinganos K. 1985. *Ap. J.* 294:397
Ferreira J, Pelletier G. 1993a. *Astron. Astrophys.* 276:625
Ferreira J, Pelletier G. 1993b. *Astron. Astrophys.* 276:637
Ferreira J, Pelletier G. 1995. *Astron. Astrophys.* 295:807
Field G. 1965. *Ap. J.* 162:531
Frank J. 1979. *MNRAS* 187:883

Frank A, Jones TW, Ryu D, Gaalaas JB. 1996. *Ap. J.* 460:777
Fukue J, Okada R. 1990. *Publ. Astron. Soc. Jpn.* 42:249
Gerwin RA. 1968. *Rev. Mod. Phys.* 40:652
Ghisellini G, Bodo G, Trussoni E, Rees MJ. 1990. *Ap. J. Lett.* 362:L1
Goldreich P, Julian WH. 1969. *Ap. J.* 157:869
Gouveia Dal Pino EM, Birkinshaw M, Benz W. 1996. *Ap. J. Lett.* 460:L111
Hardee PE, Norman ML. 1988. *Ap. J.* 334:70
Hardee PE, Norman ML. 1989. *Ap. J.* 342:6804
Hardee PE, Stone JM. 1997. *Ap. J.* 483:121
Hartman RC, Bertsch DL, Fichtel CE, Hunter SD, Kanbach G, et al. 1992. *Ap. J. Lett.* 385:L1
Heyvaerts J, Norman C. 1989. *Ap. J.* 347:1045
Icke V, Mellema G, Balick B, Eulderink F, Frank A. 1991. *Nature* 355:524
Jafelice LC, Opher R. 1992. *MNRAS* 257:135
Jennison RC, Das Gupta MK. 1953. *Nature* 172:996
Kellermann KI, Pauliny-Toth IIK. 1981. *Annu. Rev. Astron. Astrophys.* 19:373
Koide S, Nishikawa KI, Mutel RL. 1996a. *Ap. J. Lett.* 463:L71
Koide S, Sakai JI, Nishikawa KI, Mutel RL. 1996. *Ap. J.* 464:724
Koide S, Shibata K, Kudoh T. 1998. *Ap. J. Lett.* 495:L63
Komissarov SS, Falle SAEG. 1997. *MNRAS* 288:833
Königl A. 1989. *Ap. J.* 342:208
Königl A. 1994. In *Theory of Accretion Disks*, ed. WJ Duschl, J Frank, J Meyer, E Meyer-Hofmeister, WM Tscharnuter, p. 53. Dordrecht: Kluwer
Kössl D, Muller E, Hillebrandt W. 1990. *Astron. Astrophys.* 229:378, 397
Kudoh T, Shibata K. 1995. *Ap. J. Lett.* 452:L41
Kundt W. 1996. In *Jets from Stars and Galactic Nuclei*, ed. W Kundt, p. 1. Heidelberg: Springer-Verlag
Kundt W, Gopal-Krishna. 1980. *Nature* 288:149
Lacombe C. 1977. *Astron. Astrophys.* 54:1
Leahy JP, Perley RA. 1991. *Ap. J.* 344:89
Li Z, Chiueh T, Begelman MC. 1992. *Ap. J.* 394:459
Lind KR, Payne DG, Meyer DL, Blandford RD. 1989. *Ap. J.* 344:89
Loken C, Burns JO, Clarke DA, Norman ML. 1992. *Ap. J.* 392:54
Lovelace RVE. 1976. *Nature* 262:649
Lovelace RVE, Berk HL, Contopoulos J. 1991. *Ap. J.* 379:696
Lovelace RVE, Sudan RN. 1971. *Phys. Rev. Lett.* 27:1256
Lovelace RVE, Wang JCL, Sulkanen ME. 1987. *Ap. J.* 315:504
Macchetto FD. 1996. In *Extragalactic Radio Sources*, ed. R Ekers, C Fanti, L Padrielli, IAU Symp. 175, p. 195. Dordrecht: Kluwer
Macdonald D, Thorne KS. 1982. *MNRAS* 188: 345
Malagoli A, Bodo G, Rosner R. 1996. *Ap. J.* 456:708
Martì JMa, Müller E, Ibañez JMa. 1994. *Astron. Astrophys.* 281:L9
Martì JMa, Müller E, Font JA, Ibañez JMa. 1995. *Ap. J. Lett.* 448:L105
Massaglia S, Bodo G, Ferrari A. 1996a. *Astron. Astrophys.* 307:997
Massaglia S, Bodo G, Ferrari A. 1996b. In *Jets from Stars and Galactic Nuclei*, ed. W Kundt, p. 275. Heidelberg: Springer-Verlag
Mastichiadis A, Kirk JG. 1995. *Astron. Astrophys.* 295:613
Matsumoto R, Uchida Y, Hirose S, Shibata K, Hayashi MR, et al. 1996. *Ap. J.* 461:115
Meier DL. 1979. *Ap. J.* 233:664
Meier DL, Edgington S, Godon P, Payne DG, Lind KR. 1997. *Nature* 388:350
Meisenheimer K, Röser H-J, Schlötenburg M. 1996. *Astron. Astrophys.* 307:61
Mestel L. 1961. *MNRAS* 122:472
Micono M, Massaglia S, Bodo G, Rossi P, Ferrari A. 1998. *Astron. Astrophys.* 333:989
Miles JW. 1957. *J. Acoust. Soc. Am.* 29:226
Miley GK. 1980. *Annu. Rev. Astron. Astrophys.* 18:165
Miley GK, Wellington KJ, van der Laan H. 1975. *Astron. Astrophys.* 38:381
Miller RB. 1982. *An Introduction to the Physics of Intense Charged Particle Beams*. New York: Plenum
Min KW. 1997. *Ap. J.* 482:733
Mirabel IF, Rodriguez LF. 1994. *Nature* 371: 46
Moffet AT, Gubbay J, Robertson DS, Legg AJ. 1971. In *External Galaxies and Quasi-Stellar Objects*, ed. DS Evans, IAU Symp. 44, p. 228. Dordrecht: Reidel
Nishikawa K-I, Koide S, Sakai J-I, Christodoulou DM, Sol H, Mutel R. 1997. *Ap. J. Lett.* 483:L45
Nobili L, Turolla R. 1998. In *Astrophysical Jets–Open Problems, 3rd Torino Wkshp*, ed. S Massaglia, G Bodo, p. 31, Amsterdam: Gordon & Breach
Norman CA, Melrose DB, Achterberg A. 1996. *Ap. J.* 454:60
Norman ML. 1996. In *Energy Transport in Radio Galaxies and Quasars*, ed. PE Hardee, AH Bridle, JA Zensus, ASP Conf. Ser. 100, p. 319. San Francisco: Astron. Soc. Pac.
Norman ML, Balsara DS. 1993. In *Jets in Extragalactic Radio Sources*, ed. HJ Röser, K Meisenheimer, Heidelberg: Springer-Verlag
Norman ML, Burns JO, Sulkanen ME. 1988. *Nature* 335:146
Norman ML, Smarr L, Winkler K-HA, Smith MD. 1982. *Ap. J.* 113:285

Norman ML, Winkler K-HA, Smarr L. 1983. In *Astrophysical Jets*, ed. A Ferrari, AG Pacholczyk, p. 227. Dordrecht: Reidel
Ouyed R, Pudritz RE. 1997a. *Ap. J.* 482:712
Ouyed R, Pudritz RE. 1997b. *Ap. J.* 484:794
Pacholczyk AG. 1977. *Radio Galaxies*. Oxford: Pergamon
Papaloizou JCB, Lin DCN. 1995. *Annu. Rev. Astron. Astrophys.* 33:505
Parker EN. 1958. *Ap. J.* 128:664
Parker EN. 1963. *Interplanetary Dynamical Processes*. New York: Interscience
Pelletier G, Pudritz RE. 1992. *Ap. J.* 394:117
Phinney ES. 1982. In *Astrophysical Jets, 1st Torino Workshop*, ed. A Ferrari, A Pacholczyk, p. 201. Dordrecht: Reidel
Punsly B, Coroniti FV. 1990. *Ap. J.* 350:518
Qian SJ, Quirrenbach A, Witzel A, Krichbaum TP, Hummel CA, Zensus JA. 1991. *Astron. Astrophys.* 241:15
Quirrenbach A, Qian SJ, Witzel A, Krichbaum TP, Hummel CA, Alberdi S. 1989. *Astron. Astrophys.* 226:L1
Quirrenbach A, Witzel A, Wagner S, Sanchez-Pons F, Krichbaum TP, et al. 1991. *Ap. J. Lett.* 372:L71
Raga AC, Kofman L. 1992. *Ap. J.* 386:222
Rees MJ. 1971. *Nature* 229:312 (errata p. 510)
Rees MJ. 1984. *Annu. Rev. Astron. Astrophys.* 22:471
Romanova MM, Ustyugova GV, Koldoba AV, Chechetkin VM, Lovelace RVE. 1997. *Ap. J.* 482:708
Rossi P, Bodo G, Massaglia S, Ferrari A. 1993. *Ap. J.* 414:112
Rossi P, Bodo G, Massaglia S, Ferrari A. 1997. *Astron. Astrophys.* 321:672
Rosso F, Pelletier G. 1994. *Astron. Astrophys.* 287:325
Sakurai T. 1985. *Astron. Astrophys.* 152:121
Sauty C, Tsinganos K. 1994. *Astron. Astrophys.* 287:893
Scheuer PAG. 1974. *MNRAS* 166:513
Shibata K, Uchida Y. 1986. *Publ. Astron. Soc. Jpn.* 38:631
Shibata K, Uchida Y. 1990. *Publ. Astron. Soc. Jpn.* 42:39
Shu F, Najita J, Ostriker E, Wilkin F. 1994. *Ap. J.* 429:781
Sol H, Pelletier G, Asséo E. 1989. *MNRAS* 237:411
Stone JM, Norman ML. 1992. *Ap. J. Suppl.* 80: 753, 791
Stone JM, Norman ML. 1994. *Ap. J.* 433:746
Stone JM, Xu J, Hardee PE. 1997. *Ap. J.* 483: 136
Tajima T, Leboeuf JN. 1980. *Phys. Fluids* 23(5):884
Thompson PA. 1972. *Compressible Fluid Dynamics*. New York: McGraw-Hill
Trussoni E, Sauty C, Tsinganos K. 1996. In *Solar and Astrophysical MHD Flows*, ed. K Tsinganos, p. 383. Dordrecht: Kluwer
Tsinganos K, Surlantzis G, Sauty C, Trussoni E. 1996. In *Solar and Astrophysical MHD Flows*, ed. K Tsinganos, p. 427. Dordrecht: Kluwer
Turland BD. 1975. *MNRAS* 170:281, 172:181
Turland BD, Scheuer PAG. 1976. *MNRAS* 176:421
Uchida Y, Shibata K. 1985. *Publ. Astron. Soc. Jap.* 37:515
Ulrich M-H, Maraschi L, Urry CM. 1997. *Annu. Rev. Astron. Astrophys.* 35:445
Ustyugova GV, Koldoba AV, Romanova MM, Chechetkin VM, Lovelace RVE. 1995. *Ap. J. Lett.* 439:L39
van Dyke M. 1982. *An Album of Fluid Motion*. Stanford: Parabolic
van Putten MHPM. 1996. *Ap. J. Lett.* 467:L57
Villata M, Ferrari A. 1995. *Astron. Astrophys.* 293:626
Weber EJ, Davis L. 1967. *Ap. J.* 148:217
Whitney AR, Shapiro II, Rogers AAE, Robertson DS, Knight CA, et al. 1971. *Science* 173:225
Witzel A. 1992. In *Physics of Active Galactic Nuclei*, ed. WJ Duschl, SJ Wagner, p. 484. Berlin: Springer-Verlag
Zachary AL, Malagoli A, Colella P. 1994. *SIAM J. Sci. Comp.* 15:263
Zensus JA. 1996. In *Extragalactic Radio Sources*, IAU Symp. 175, p. 5. Dordrecht: Kluwer